Supporting information

Microcrystalline solid-solid transformations of conformationally-responsive solvates, desolvates and a salt of *N,N′*-(1,4-phenylene)dioxalamic acid: the energetics of hydrogen bonding and n/π→π* interactions

Marcos Morales-Santana[†], *Sayuri Chong-Canto*[†], *José Martín Santiago-Quintana*[†], *Francisco J. Martínez-Martínez*[§], *Efrén V. García-Báez*[†*], *Alejandro Cruz*[†], *Susana Rojas-Lima*[‡], *Itzia I. Padilla-Martínez*[†*]

† Laboratorio de Química Supramolecular y Nanociencias, Instituto Politécnico Nacional-UPIBI, Av. Acueducto s/n Barrio la Laguna Ticomán, Ciudad de México, C.P. 07340, Mexico

§ Facultad de Ciencias Químicas, Universidad de Colima, Km. 9 Carretera Colima-Coquimatlán, C.P. 28400, Coquimatlán, Colima, Mexico

‡ Área Académica de Química, Universidad Autónoma del Estado de Hidalgo, Carretera Pachuca-Tulancingo Km. 4.5, Ciudad Universitaria, C.P. 42184, Mineral de la Reforma, Hidalgo, Mexico

List of contents:

1. Detailed experimental section

1.1 Materials and crystals. All reagents and solvents were of analytical grade and used as received.

N,N'-(1,4-phenylene)dioxalamic acid double-hydrate I (H_2pOx·2W, W = water, hydromorph H-I). A suspension of *N,N'*-(1,4-phenylene)dioxalamic acid diethylester (2.00 g, 6.487 mmol) and NaOH (0.572 g, 14.30 mmol) in 35 mL of methyl alcohol was refluxed for 4 h. The solid was filtered, suspended in 100 mL of distilled water and acidified with concentrated HCl until pH = 1.0. The precipitated pale beige solid was filtered, washed with distilled water and dried at RT to yield 1.48 g of H-I (5.14 mmol, 90%).

N,N'-(1,4-phenylene)dioxalamic acid double-hydrate II (H-II). A suspension of 100 mg of H-I and 20 mL of distilled water were boiled at 92 °C under stirring until complete dissolution, if necessary 1-2 mL of extra water are added. The resulting solution was left to cool to room temperature and after 20 min a pale pearl beige microcrystalline solid appeared; it was filtered and dried at RT for 24 h.

N,N'-(1,4-phenylene)dioxalamic acid anhydrate I (A-I). Obtained by dehydration of 500 mg of H-I in an air driven oven at 150 °C for 3 h.

N,N'-(1,4-phenylene)dioxalamic acid anhydrate II (A-II). Obtained as described for A-I, starting from H-II.

N,N'-(1,4-phenylene)dioxalamic acid anhydrate III (A-III). Obtained by desolvation of 200 mg of H_2pOx·2DMSO prepared by grinding procedure or large crystals of H_2pOx·2DMF, in an air driven oven at 160 °C for 24 h.

N,N'-(1,4-phenylene)dioxalamic acid di-(dimethyl sulfoxide) (H_2pOx·2DMSO). 200 mg (0.694 mmol) of H-I and 700 μl (6.94 mmol) of DMSO were grinded with a pestle in a mortar for 30 min, the resulting sticky paste was left to evaporate at RT for 24 h, then washed with two portions of diethyl ether (5 mL each) and dried at RT until a dry microcrystalline solid appeared (0.280 g). Single crystals of H_2pOx·2DMSO were grown boiling 200 mg of H-I in 4.0 mL of DMSO, after 24 h of cooling to RT, crystals of H_2pOx·2DMSO appeared.

N,N'-(1,4-phenylene)dioxalamic acid di-(dimethyl formamide) (H_2pOx·2DMF). 600 mg (2.082 mmol) of H-I and 1.5 mL of DMF were grinded with a pestle in a mortar to obtain a dry solid

phase. Single crystals of H_2pOx·2DMF were grown from 530 mg (1.839 mmol) of H-I in 10.0 mL of DMF at RT. After 12 days 330 mg (0.828 mmol) of amber crystals were cropped by filtration. Further crops yielded 126 mg of dimethyl ammonium salt $(HDMA)_2$pOx.

Tri-(N,N'-(1,4-phenylene)dioxalamic acid) di-(methyl alcohol) tetrahydrate ($3H_2$pOx·2MeOH·4W). 200 mg (0.694 mmol) of H-I and 80.0 mL of methyl alcohol were boiled until complete dissolution. The mixture was cooled to RT and 80.0 mL of distilled water were added, single crystals appeared after one week (100 mg).

N,N'-(1,4-phenylene)dioxalamate di-(dimethyl ammonium) ($(HDMA)_2$pOx). 2.00 g (6.95 mmol) of H-I, 20 mL of DMF and 5.0 mL of distilled water were refluxed during 1.0 h, after filtration 1.366 g (4.00 mmol) of crystalline pink solid were obtained. Single crystals of $(HDMA)_2$pOx were grown from saturated aqueous solution at RT.

1.2 Instrumental. IR spectra were recorded neat at 25 °C using a Perkin Elmer Spectrum GX series with FT system spectrophotometer using the ATR device. ^{13}C CPMAS spectra were recorded on a Bruker Avance DPX-400 (101 MHz). The following conditions were applied: spectral width 30.242 kHz, acquisition time 33.8 ms, contact time 2000 ms, rotation rate 8 kHz, relaxation delay 5 s, and up to 256 scans for each spectrum were collected. Room temperature X-ray powder diffraction data were collected on a PAN Analytical X'Pert PRO diffractometer with Cu Kα1 radiation (λ = 1.5405 Å, 45 kV, 40 mA) or on a D8 Focus Bruker AXS instrument using Cu Kα1 radiation (λ = 1.542 Å, 35 kV, 25 mA). DSC and TG measurements were performed in a Q2000 equipment and a Thermobalance Q5000 IR, respectively, of TA instruments. In both cases, approximately 3.0-5.0 mg of sample was used and a gradient of 5.00 °C/min from room temperature to 350 °C under air flux of 50 mL/min in an open (TG) or pin-holed panels (DSC).

1.3 X-Ray structure determination. Crystal data, collection, and refinement parameters are listed in Table 1. Single crystal X-ray diffractions data were collected on an Agilent SuperNova (dual source) diffractometer equipped with graphite-monochromatic Cu (λ = 1.54184 Å)/Mo (λ = 0.71073 Å) Kα radiation. The data collection was accomplished using CrysAlisPro software[1] at 293 K under the Cu (H_2pOx·2DMSO)/Mo (H_2pOx·2DMF, $3H_2$pOx·2MeOH·4W, $(HDMA)_2$pOx) Kα radiation. The cell refinement and data reduction were carried out with the CrysAlisPro software[1]. The models were refined and the structures solved (direct methods) using the SHELXL-2018/3 program[2] of the WINGX package[3]. The H atoms on C, N, and O were geometrically

positioned and treated as riding atoms with: C−H 0.93−0.96 Å, Uiso(H) = 1.2 eq(C) for aromatic carbon atoms or 1.5 eq(C) for methyl carbon atoms; O−H = 0.82 Å, Uiso(H) = 1.5 eq(O); N−H = 0.86 Å, Uiso(H) = 1.2 eq(N) for $3H_2pOx{\cdot}2MeOH{\cdot}4W$. The H atoms on C were treated as already described but H atoms on O and N were found by Fourier differences and freely refined for $H_2pOx{\cdot}2DMSO$, $H_2oOx{\cdot}2DMF$ and $(HDMA)_2pOx$. Platon[4] and Mercury[5] were used to prepare the material for publication. Hydrogen bonding motifs were described following standard notation[6]. The CIF codes deposited at the CCDC are $H_2pOx{\cdot}2DMSO$ (1874282), $H_2pOx{\cdot}2DMF$ (1997487), $3H_2pOx{\cdot}2MeOH{\cdot}4W$ (1997485) and $(HDMA)_2pOx$ (1997486).

1.4 Hirshfeld surface (HS)[7,8], two-dimensional fingerprint plots[9] and energy-framework diagrams[10]. These calculations and energy-framework diagrams were performed in the software CrystalExplorer17.5[11]. The HS was mapped over d_{norm}, and the function of normalized contact distance, d_e and d_i was utilized, where d_e and d_i are the distance from a given point to the nearest atom outside and inside on the surface, respectively[12]. The colors of the d_{norm} –mapped HS represent the interatomic contacts as the distances longer tan de sum of van der Waals radii (white to blue) or distances shorter than the sum of the van der Waals radii (red). The energy-framework diagrams are represented by cylinders that join the centroids of multiple molecular pairs. The radius of the cylinder is proportional to the magnitude of the interaction energy. The energy components like electrostatic potential forces, E_{elect} (red), dispersion forces, E_{disp} (green), and total energy, E_{total} (blue), were obtained with the calculation of the wave function of each solvate linking the CrystalExplorer17.5 software with the Gaussian 09 software[13] using the B3LYP/6-31G (d,p) level of theory and then were adjusted to the same scale factor of 80 with a cut-off value of 9.7 kJ mol^{-1} within a 3.8 Å radius about a central molecule. Scale factors[11] $k_{ele} = 1.057$, $k_{pol} = 0.740$, $k_{dis} = 0.871$, $k_{rep} = 0.618$ were used for E_{tot} calculation. The % contribution of individual component to the stabilization energy was calculated through $(E_{comp}/(E_{stab})*100$, where $E_{stab} = E_{ele} + E_{pol} + E_{disp}$[14].

1.5. *Lattice energy*. The lattice energy calculation was performed in the CLP-PIXEL software (Gavezzotti, 2003, 2005)[15,16]. Each *CIF* file for the co-crystals was converted into *OIH* and *OEH* files using the *Retcif* module for the renormalization of the H atoms in the structure, the *Retcor* module was used for checking subgroups in the space group, the *Retcha* module assigned atomic point charges in the structure and finally the *Clpcry* module calculate the contributions of energy that provide the total lattice energy per fragment in the co-crystal. All modules used for the

calculation were available for the atom-atom approach (AA-CLP) software (Gavezzotti, 2013)[17], in which the evaluation of the total lattice energy only require cell dimensions and atomic nuclear coordinates.

2. Crystal data, collection and refinement

Table S1. Crystal data, collection and refinement parameters of $H_2pOx{\cdot}2S$ (S = DMSO, DMF, ⅓(MeOH·2W)) and $(HDMA)_2pOx$ salt.

	$H_2pOx{\cdot}2DMSO$	$H_2pOx{\cdot}2DMF$	$3H_2pOx{\cdot}2MeOH{\cdot}4W$	$(HDMA)_2pOx$
Chemical formula	$C_{10}H_8N_2O_6{\cdot}2(C_2H_6SO)$	$C_{10}H_8N_2O_6{\cdot}2(C_3H_7NO)$	$3(C_{10}H_8N_2O_6){\cdot}2(CH_4O){\cdot}4(H_2O)$	$C_{10}H_6N_2O_6{\cdot}2(C_2H_8N)$
M_r	408.44	398.38	892.70	342.36
Crystal system	Monoclinic	Monoclinic	Triclinic	Monoclinic
Space group	$P2_1/c$	$P2_1/c$	P-1	$P2_1/n$
a, b, c (Å)	7.6501(2), 11.8612(4), 10.4802(3)	7.0616(4), 12.9600(6), 10.6639(4)	9.5470(8), 10.2921(9), 11.4084(11)	5.9712(3), 7.0040(3), 20.4618(9)
α, β, γ (°)	90.0, 98.090(3), 90.0	90.0, 94.752(4), 90.0	70.436(9), 66.208(9), 86.296(7)	90.0, 98.336(4), 90.0
V (Å^3)	941.50 (5)	972.59 (8)	963.26 (18)	846.72 (7)
Z	2	2	1	2
Dcalc (g/cm^3)	1.441	1.360	1.534	1.343
Crystal size (mm)	0.40×0.33×0.30	0.20×0.22×0.40	0.20×0.25×0.30	0.35×0.45×0.55
No. of meas, indep, obs [$I > 2\sigma(I)$] reflections	9168, 1881, 1584	43245, 2686, 2022	29987, 5069, 2474	29486, 2340, 2016
R_{int}	0.031	0.043	0.076	0.026
$R[F^2 > 2\sigma(F^2)]$, $wR(F^2)$, S	0.041, 0.115, 1.05	0.043, 0.108, 1.036	0.065, 0.157, 0.996	0.037, 0.096, 1.054

3. PXRD

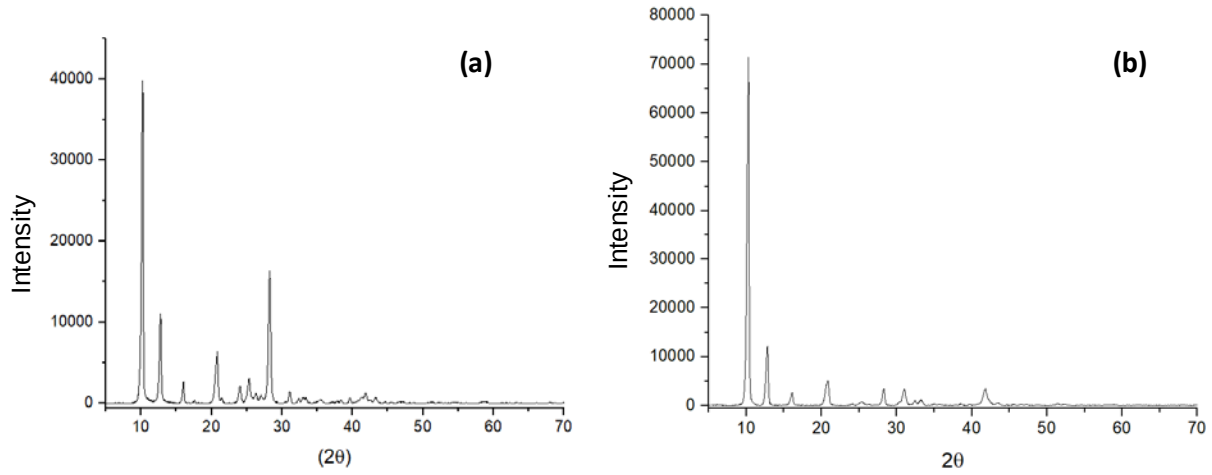

Figure S1. PXRD patterns of anhydrates A-I (a) and A-II and (b), former (g) and (h) in Figure 2 of the main text.

4. Molecular and supramolecular structures

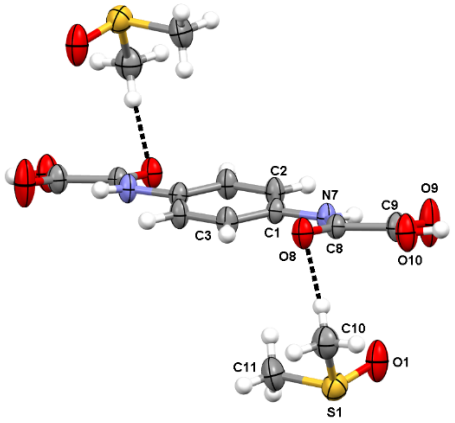

Figure S2. The molecular structure of H_2pOx·2DMSO cocrystal, showing the atom labelling scheme. Displacement ellipsoids are drawn at the 50% probability level.

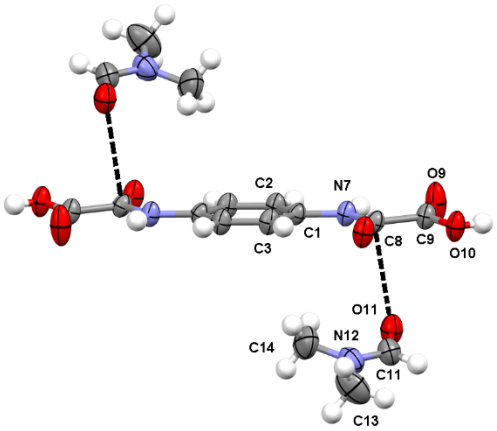

Figure S3. The molecular structure of H_2pOx·2DMF cocrystal solvate, showing the atom labelling scheme. Displacement ellipsoids are drawn at the 50% probability level.

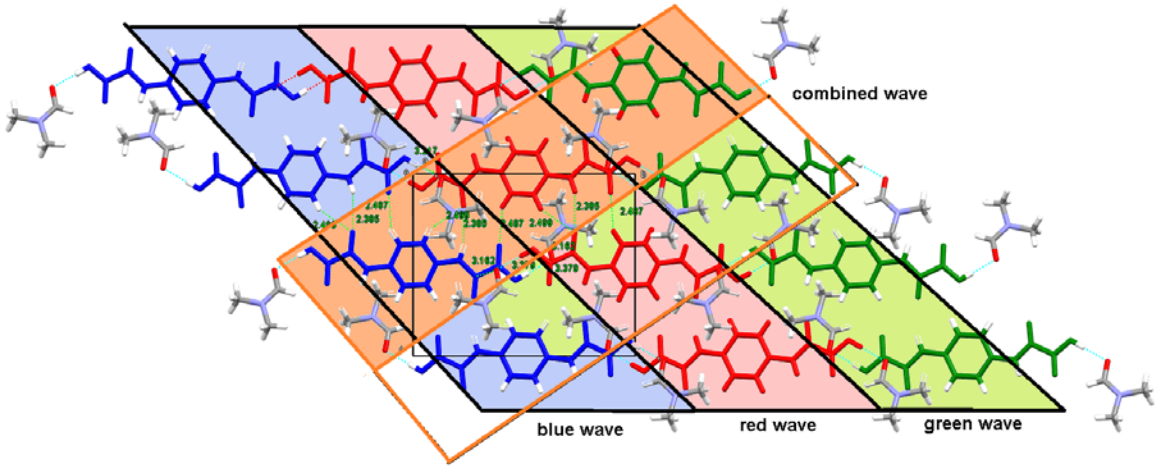

Figure S4. The supramolecular structure of H_2pOx·2DMF cocrystal solvate.

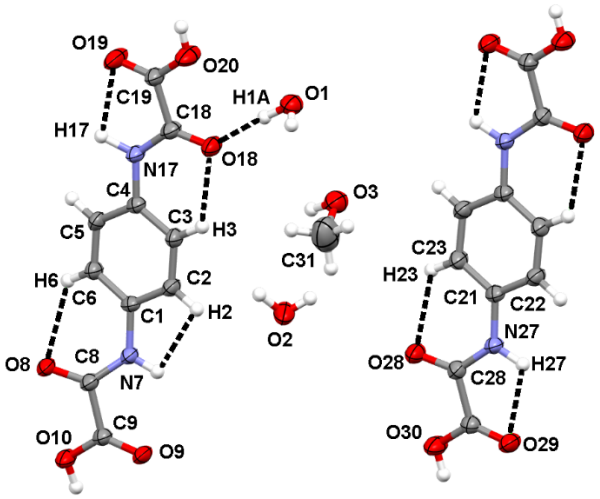

Figure S5. The molecular structure of $3H_2pOx{\cdot}2MeOH{\cdot}4W$ cocrystal solvate, showing the atom labelling scheme. Displacement ellipsoids are drawn at the 50% probability level.

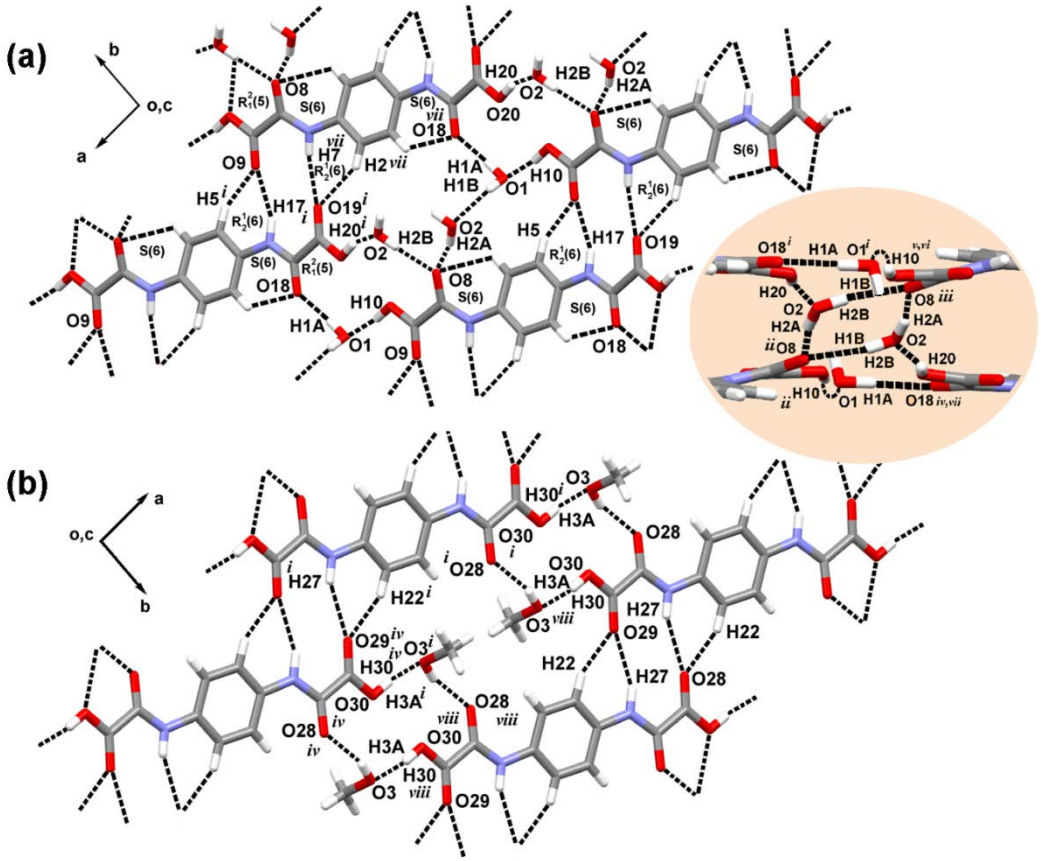

Figure S6. Supramolecular architecture of $3H_2POx{\cdot}2MeOH{\cdot}4W$. (a) Hydrogen bonded aqueous monolayer in the (0 0 1) family of planes; a detail of the hydrogen bonding pattern between two antiparallel aqueous layers is shown in the insert. (b) Hydrogen bonding scheme of the methanol monolayer in the (0 0 -1) family of planes. See Table 6 for geometric parameters and symmetry codes.

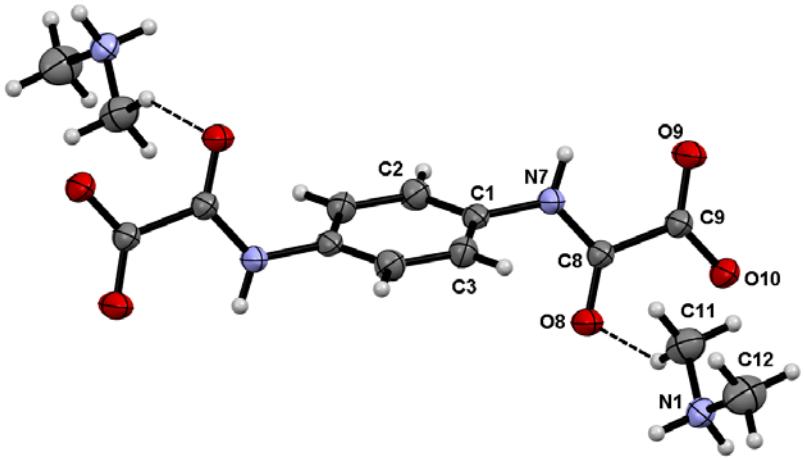

Figure S7. The molecular structure of $(HDMA)_2pOx$ salt, showing the atom labelling scheme. Displacement ellipsoids are drawn at the 50% probability level.

Table S2. Selected geometric parameters of $H_2pOx{\cdot}2DMSO$.

C1—C2	1.387 (3)	C8—C9	1.543 (3)
C1—C3	1.392 (3)	C9—O9	1.193 (2)
C1—N7	1.418 (2)	C9—O10	1.298 (2)
C2—C3^{i}	1.381 (3)	C10—S1	1.776 (3)
C3—C2^{i}	1.381 (3)	C11—S1	1.782 (3)
C8—O8	1.212 (2)	O1—S1	1.5172 (18)
C8—N7	1.342 (2)		
C2—C1—C3	119.05 (17)	O9—C9—O10	126.11 (19)
C2—C1—N7	117.68 (16)	O9—C9—C8	121.70 (17)
C3—C1—N7	123.27 (16)	O10—C9—C8	112.19 (17)

C3^{i}—C2—C1	121.31 (18)	C8—N7—C1	127.15 (16)
C2^{i}—C3—C1	119.64 (17)	O1—S1—C10	106.17 (12)
O8—C8—N7	126.56 (17)	O1—S1—C11	104.06 (11)
O8—C8—C9	121.87 (16)	C10—S1—C11	98.70 (13)
N7—C8—C9	111.57 (16)		
C3—C1—C2—C3^{i}	0.4 (4)	O8—C8—C9—O10	−2.7 (3)
N7—C1—C2—C3^{i}	−179.43 (19)	N7—C8—C9—O10	176.61 (18)
C2—C1—C3—C2^{i}	−0.4 (3)	O8—C8—N7—C1	4.0 (3)
N7—C1—C3—C2^{i}	179.42 (19)	C9—C8—N7—C1	−175.27 (18)
O8—C8—C9—O9	176.9 (2)	C2—C1—N7—C8	168.12 (19)
N7—C8—C9—O9	−3.8 (3)	C3—C1—N7—C8	−11.7 (3)

Symmetry code: (i) −*x*, −*y*+1, −*z*+1.

Table S3. Hydrogen bonding and n→π* geometric parameters of H_2pOx·2DMSO.

D—H···*A*	*D*—H	H···*A*/Å	*D*···*A*/Å	*D*—H···*A*/°
N7—H7···O9	0.77(2)	2.29(2)	2.677(2)	113(2)
N7—H7···O8^{i}	0.77(2)	2.42(2)	3.102 (2)	150(2)
C2—H2···O8^{i}	0.93	2.47	3.234 (2)	139
C3—H3···O8	0.93	2.28	2.875(2)	121
C3—H3···O9^{ii}	0.93	2.49	3.332 (2)	150
C10—H10*A*···O1^{ii}	0.96	2.51	3.442 (3)	164
C10—H10*B*···O8	0.96	2.46	3.373 (3)	159
C10—H10*C*···O9^{iii}	0.96	2.58	3.353 (3)	137
O10—H10···O1^{iii}	0.87(3)	1.71(3)	2.561 (2)	165(3)
O10—H10···S1^{iii}	0.87(3)	2.75(3)	3.5928(17)	163(3)
C11—H11B··· Cg^{iv,v}	0.96	2.87	3.648(3)	139
X—O···C			O···C	X—O···C
S1—O1···C9			3.381(2)	123.6(1)
O1—S1···C8^{iv}			3.693(2)	100.2(1)

Symmetry codes: (i) *x*, −*y*+1/2, *z*+1/2; (ii) *x*, −*y*+1/2, *z*−1/2; (iii) −*x*+1, −*y*, −*z*+1; (iv) 1+*x*, *y*, *z*; (v) 1−*x*, 1−*y*, 1−*z*

Table S4. Selected geometric parameters of H_2pOx·2DMF.

O8—C8	1.2146 (14)	C2—C3^{i}	1.3791 (17)
O9—C9	1.2004 (15)	C8—C9	1.5350 (17)
O10—C9	1.2961 (14)	O11—C11	1.2299 (19)
N7—C8	1.3435 (14)	N12—C11	1.317 (2)
N7—C1	1.4140 (15)	N12—C14	1.444 (3)
C1—C3	1.3882 (15)	N12—C13	1.446 (2)
C1—C2	1.3890 (16)		
C8—N7—C1	128.65 (10)	N7—C8—C9	110.70 (9)
C3—C1—C2	119.37 (11)	O9—C9—O10	125.81 (12)
C3—C1—N7	123.28 (10)	O9—C9—C8	120.44 (11)
C2—C1—N7	117.36 (10)	O10—C9—C8	113.73 (10)
C3^{i}—C2—C1	120.96 (11)	C11—N12—C14	122.19 (16)
C2^{i}—C3—C1	119.67 (10)	C11—N12—C13	120.77 (18)
O8—C8—N7	127.07 (11)	C14—N12—C13	117.03 (17)
O8—C8—C9	122.21 (10)		
C8—N7—C1—C3	2.84 (19)	C1—N7—C8—C9	−178.04 (11)
C8—N7—C1—C2	−177.25 (12)	O8—C8—C9—O9	−173.69 (14)
C3—C1—C2—C3^{i}	−0.6 (2)	N7—C8—C9—O9	4.86 (19)
N7—C1—C2—C3^{i}	179.48 (12)	O8—C8—C9—O10	4.71 (19)
C2—C1—C3—C2^{i}	0.6 (2)	N7—C8—C9—O10	−176.74 (11)
N7—C1—C3—C2^{i}	−179.49 (12)	C14—N12—C11—O11	−0.7 (3)
C1—N7—C8—O8	0.4 (2)	C13—N12—C11—O11	−179.95 (18)

Symmetry code: (i) −*x*, −*y*+1, −*z*.

Table S5. Hydrogen bonding and n→π* geometric parameters of H_2pOx·2DMF.

D—H···*A*	*D*—H	H···*A*/Å	*D*···*A*/Å	*D*—H···*A*/°
N7—H7···O9	0.825(16)	2.199(15)	2.6295(14)	112.7(13)
N7—H7···O8^{ii}	0.825(16)	2.423(16)	3.2132 (13)	160.8(14)
O10—H10···O11^{i}	0.94(2)	1.64(2)	2.5791(14)	174(2)

C11—H11···O9^{i}	0.93	2.33	3.0509 (18)	134
C3—H3···O8	0.93	2.31	2.9181(15)	122
C2—H2···O8^{ii}	0.93	2.50	3.3363 (15)	150
C3—H3···O9^{iii}	0.93	2.49	3.3044 (16)	147
C—O···C			O···C	C—O···C
C11—O11···C8^{iv}			3.162(2)	108.5(2)
C9—O10···C11			3.316(2)	86.61(2)

Symmetry codes: (i) 1−*x*, −*y*, 1−*z*; (ii) *x*, ½−*y*, ½+*z*; (iii) *x*, ½−*y*, −½+*z*; (iv) 1+*x*, *y*, *z*;

Table S6. Selected geometric parameters of $3H_2$pOx·2MeOH·4W.

O8—C8	1.230 (3)	C4—C5	1.381 (3)
O9—C9	1.208 (3)	C8—C9	1.542 (3)
O10—C9	1.287 (3)	C18—C19	1.540 (3)
O18—C18	1.221 (3)	O28—C28	1.219 (3)
O20—C19	1.302 (3)	O29—C29	1.201 (3)
O19—C19	1.194 (3)	O30—C29	1.300 (3)
N7—C8	1.331 (3)	N27—C28	1.332 (3)
N7—C1	1.422 (3)	N27—C21	1.425 (3)
N17—C18	1.328 (3)	C21—C22	1.385 (3)
N17—C4	1.426 (3)	C21—C23	1.388 (3)
C1—C2	1.384 (3)	C22—C23^{i}	1.383 (3)
C1—C6	1.388 (3)	C28—C29	1.540 (3)
C2—C3	1.382 (3)	O3—C31	1.422 (4)
C3—C4	1.387 (3)		
C8—N7—C1	127.14 (19)	O18—C18—N17	127.0 (2)
C18—N17—C4	127.65 (19)	O18—C18—C19	120.5 (2)
C2—C1—C6	119.6 (2)	N17—C18—C19	112.5 (2)
C2—C1—N7	117.52 (19)	O19—C19—O20	126.1 (2)
C6—C1—N7	122.8 (2)	O19—C19—C18	122.8 (2)
C3—C2—C1	120.5 (2)	O20—C19—C18	111.1 (2)
C5—C4—C3	119.6 (2)	C28—N27—C21	127.35 (19)
C5—C4—N17	117.7 (2)	C22—C21—C23	119.2 (2)
C3—C4—N17	122.7 (2)	C22—C21—N27	117.7 (2)
C6—C5—C4	120.8 (2)	C23—C21—N27	123.1 (2)

O8—C8—N7	126.2 (2)	C23^{i}—C22—C21	120.9 (2)
O8—C8—C9	120.8 (2)	C22^{i}—C23—C21	119.8 (2)
N7—C8—C9	112.93 (19)	O28—C28—N27	126.5 (2)
O9—C9—O10	127.1 (2)	H31A—C31—H31C	109.5
O9—C9—C8	121.5 (2)	H31B—C31—H31C	109.5
O10—C9—C8	111.45 (19)		
C8—N7—C1—C2	160.6 (2)	C4—N17—C18—O18	4.0 (5)
C8—N7—C1—C6	−21.2 (4)	C4—N17—C18—C19	−174.3 (2)
C6—C1—C2—C3	3.1 (4)	O18—C18—C19—O19	177.9 (3)
N7—C1—C2—C3	−178.7 (2)	N17—C18—C19—O19	−3.7 (4)
C1—C2—C3—C4	0.5 (4)	O18—C18—C19—O20	−4.1 (4)
C2—C3—C4—C5	−3.1 (4)	N17—C18—C19—O20	174.2 (2)
C2—C3—C4—N17	176.8 (2)	C28—N27—C21—C22	173.3 (2)
C18—N17—C4—C5	−176.3 (2)	C28—N27—C21—C23	−8.2 (4)
C18—N17—C4—C3	3.8 (4)	C23—C21—C22—C23^{i}	−0.5 (4)
C4—C5—C6—C1	1.5 (4)	N27—C21—C22—C23^{i}	178.0 (2)
C2—C1—C6—C5	−4.0 (4)	C22—C21—C23—C22^{i}	0.5 (4)
N7—C1—C6—C5	177.8 (2)	N27—C21—C23—C22^{i}	−177.9 (2)
C1—N7—C8—O8	−3.2 (4)	C21—N27—C28—O28	−5.6 (4)
C1—N7—C8—C9	178.0 (2)	C21—N27—C28—C29	175.0 (2)
O8—C8—C9—O9	−165.2 (2)	O28—C28—C29—O29	−173.9 (3)
N7—C8—C9—O9	13.7 (4)	N27—C28—C29—O29	5.4 (4)
O8—C8—C9—O10	14.1 (3)	O28—C28—C29—O30	7.3 (4)
N7—C8—C9—O10	−167.0 (2)	N27—C28—C29—O30	−173.3 (2)

Table S7. Hydrogen bonding and n→π* geometric parameters of $3H_2$pOx·2MeOH·4W.

D—H···*A*	*D*—H	H···*A*/Å	*D*···*A*/Å	*D*—H···*A*/°
N27—H27···O29	0.86	2.30	2.706(2)	109
N7—H7···O19^{v}	0.86	2.22	3.018(2)	154
N17—H17···O9^{vii}	0.86	2.25	3.068(2)	159
N27—H27···O29^{ix}	0.86	2.29	3.102(3)	158
C3—H3···O18	0.93	2.26	2.872(3)	123
C6—H6···O8	0.93	2.38	2.908(3)	116
O1—H1A···O18^{i}	0.92	1.89	2.808(2)	176

O1—H1B···O2^{ii}	0.79	2.20	2.975(3)	166
O2—H2A···O8^{iii}	0.94	1.99	2.913(3)	167
O2—H2B···O8^{iv}	0.81	1.99	2.791(2)	171
O10—H10···O1^{vi}	0.87	1.70	2.561(2)	168
O20—H20···O2^{vii}	0.82	1.86	2.629(2)	155
C23—H23···O28	0.93	2.29	2.877(3)	121
O3—H3A···O28^{viii}	0.82	1.99	2.772(2)	159
O30—H30···O3^{v}	0.82	1.76	2.571(2)	168
C2—H2···O19^{v}	0.93	2.44	3.241(3)	145
C5—H5···O9^{vii}	0.93	2.53	3.304(3)	141
C22—H22···O29^{ix}	0.93	2.52	3.292 (3)	141

C—O···C	O···C	C—O···C
C9—O9···C18^{iii}	3.194(2)	87.2(2)
C18—O18···C9^{iii}	3.168(2)	88.2(2)

Symmetry codes: (i) *x*, *y*, *z*¸ (ii) 1−*x*, 1−*y*, −*z*; (iii) 1−*x*, 2−*y*, −*z*; (iv) 1+*x*, 1+*y*, *z*; (v) 1+*x*, *y*, *z*; (vi) x, −1+y, z; (vii) −1+*x*, *y*, *z*; (viii) 1−*x*, 1−*y*, 1−*z*; (ix) 2−*x*, −*y*, 1−*z*.

Table S8. Selected geometric parameters of $(HDMA)_2pOx$.

C1—C6	1.3783 (15)	C8—C9	1.5479 (13)
C1—C2	1.3804 (14)	C9—O9	1.2274 (12)
C1—N7	1.4267 (12)	C9—O10	1.2480 (12)
C2—C6^{i}	1.3869 (14)	C11—N1	1.4701 (15)
C8—O8	1.2199 (12)	C12—N1	1.4676 (15)
C8—N7	1.3346 (12)		
C6—C1—C2	120.24 (9)	N7—C8—C9	114.05 (8)
C6—C1—N7	120.31 (9)	O9—C9—O10	127.36 (9)
C2—C1—N7	119.44 (9)	O9—C9—C8	118.35 (8)
C1—C2—C6^{i}	119.90 (10)	O10—C9—C8	114.29 (8)
C1—C6—C2^{i}	119.86 (10)	C12—N1—C11	113.10 (10)
O8—C8—N7	124.81 (9)	C8—N7—C1	123.48 (8)
O8—C8—C9	121.13 (8)		

C6—C1—C2—C6^{i}	−0.46 (17)	O8—C8—C9—O10	−1.07 (16)
N7—C1—C2—C6^{i}	178.01 (9)	N7—C8—C9—O10	178.08 (10)
C2—C1—C6—C2^{i}	0.46 (17)	O8—C8—N7—C1	−1.33 (17)
N7—C1—C6—C2^{i}	−178.00 (9)	C9—C8—N7—C1	179.56 (9)
O8—C8—C9—O9	179.66 (11)	C6—C1—N7—C8	−68.37 (14)
N7—C8—C9—O9	−1.19 (15)	C2—C1—N7—C8	113.16 (12)

Symmetry code: (i) −*x*+2, −*y*+1, −*z*+1.

Table S9. Hydrogen bonding geometric parameters of $(HDMA)_2pOx$.

D—H···*A*	*D*—H	H···*A*/Å	*D*···*A*/Å	*D*—H···*A*/°
N7—H7···O9^{i}	0.858(15)	2.302(14)	2.6784(13)	106.8(12)
N1—H1AB···O10^{ii}	0.950(13)	1.767(13)	2.7158(13)	176.3(12)
N1—H1A···O8^{iii}	0.889(14)	2.311(14)	2.9951(12)	133.7(11)
N1—H1A···O10^{iii}	0.889(14)	2.005(14)	2.8062(12)	149.2(12)
N7—H7···O9^{iv}	0.859(16)	2.061(16)	2.8460(12)	151.8(14)
C11—H11A···O8^{i}	0.96	2.58	3.4290(15)	148
C11—H11B···Cg^{v}	0.96	2.84	3.6071(13)	138

Symmetry codes: (i) *x*, *y*, *z*; (ii) *x*, -1+*y*, *z*; (iii) ½-*x*, -1/2+*y*, ½-*z*; (iv) 1-x, 2 - y, 1-z; (v) *1-x*, *y*, *z*.

5. Theoretical calculations.

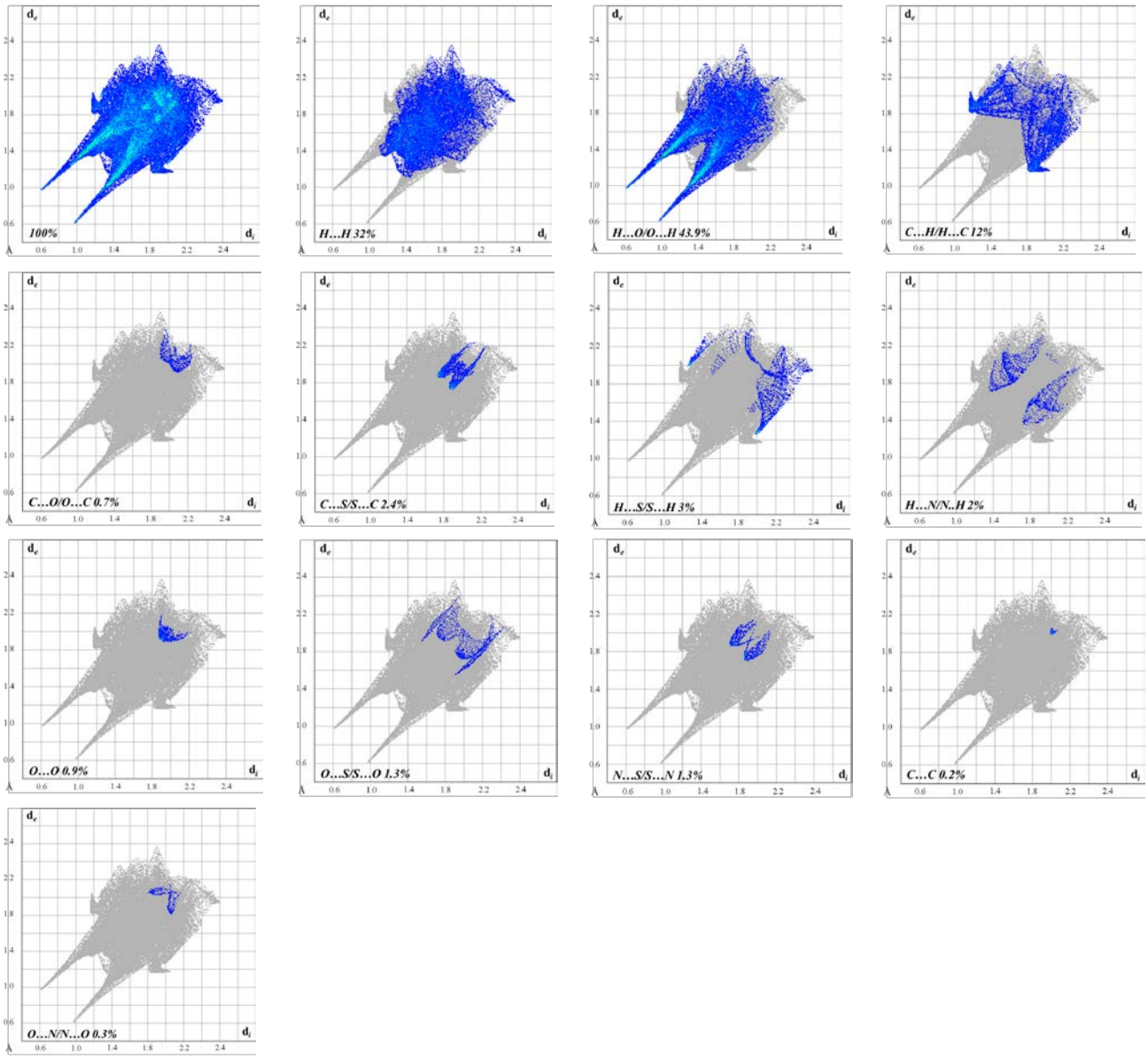

Figure S8. 2D finger print plots of H_2pOx·2DMSO.

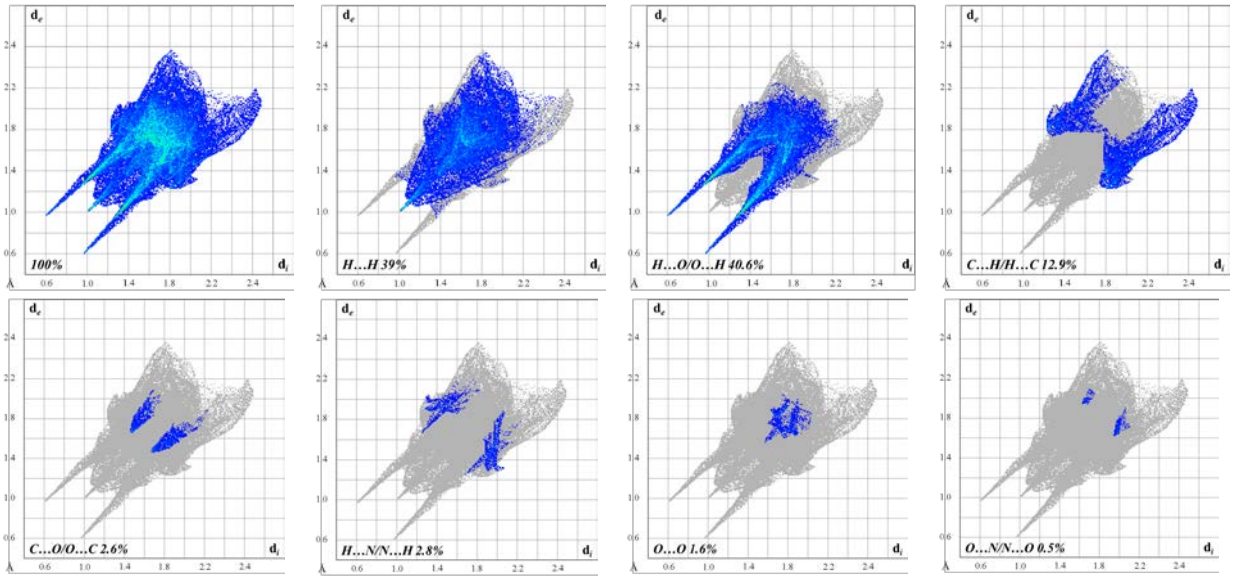

Figure S9. 2D finger print plots of H_2pOx·2DMF.

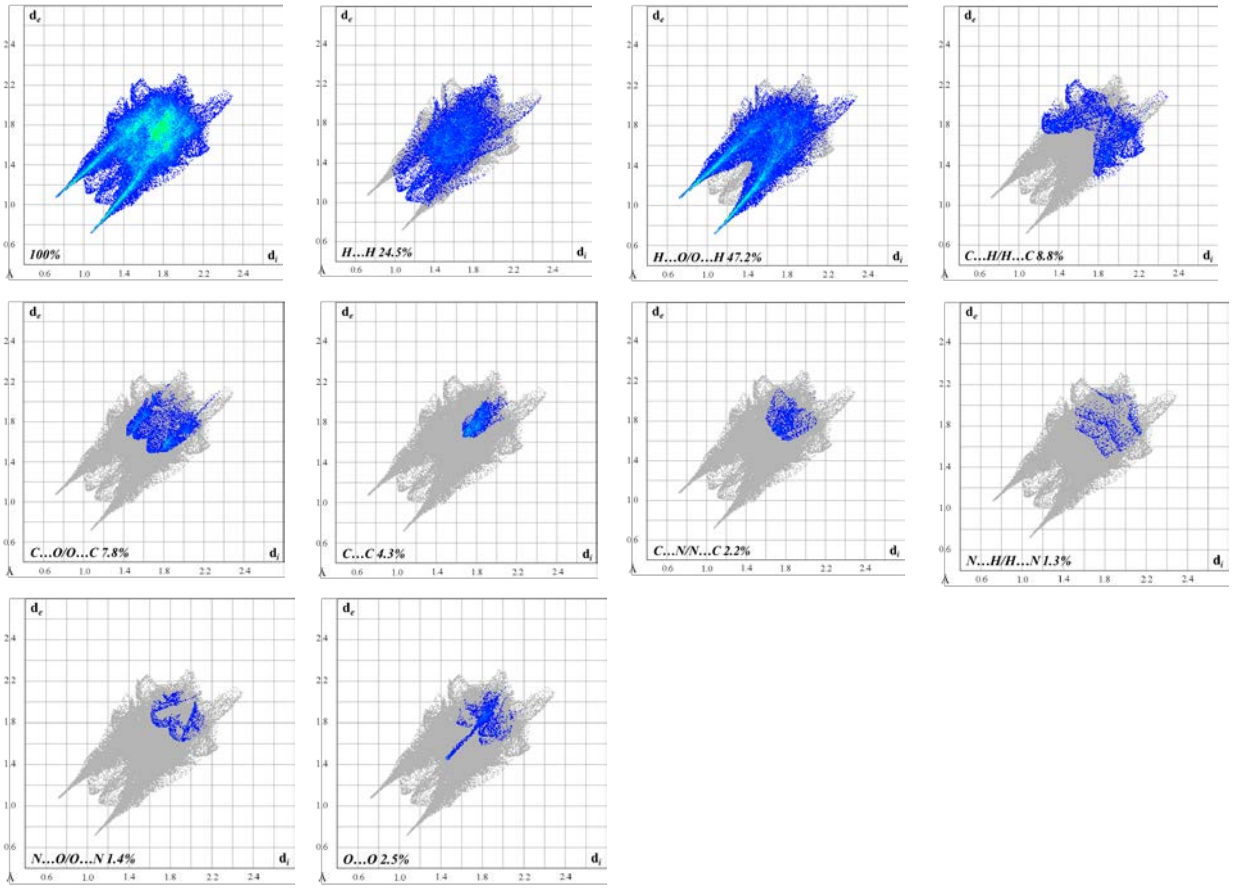

Figure S10. 2D finger print plots of the aqueous bilayer $(H_2pOx·2W)_2$ of $3H_2pOx·2MeOH·4W$.

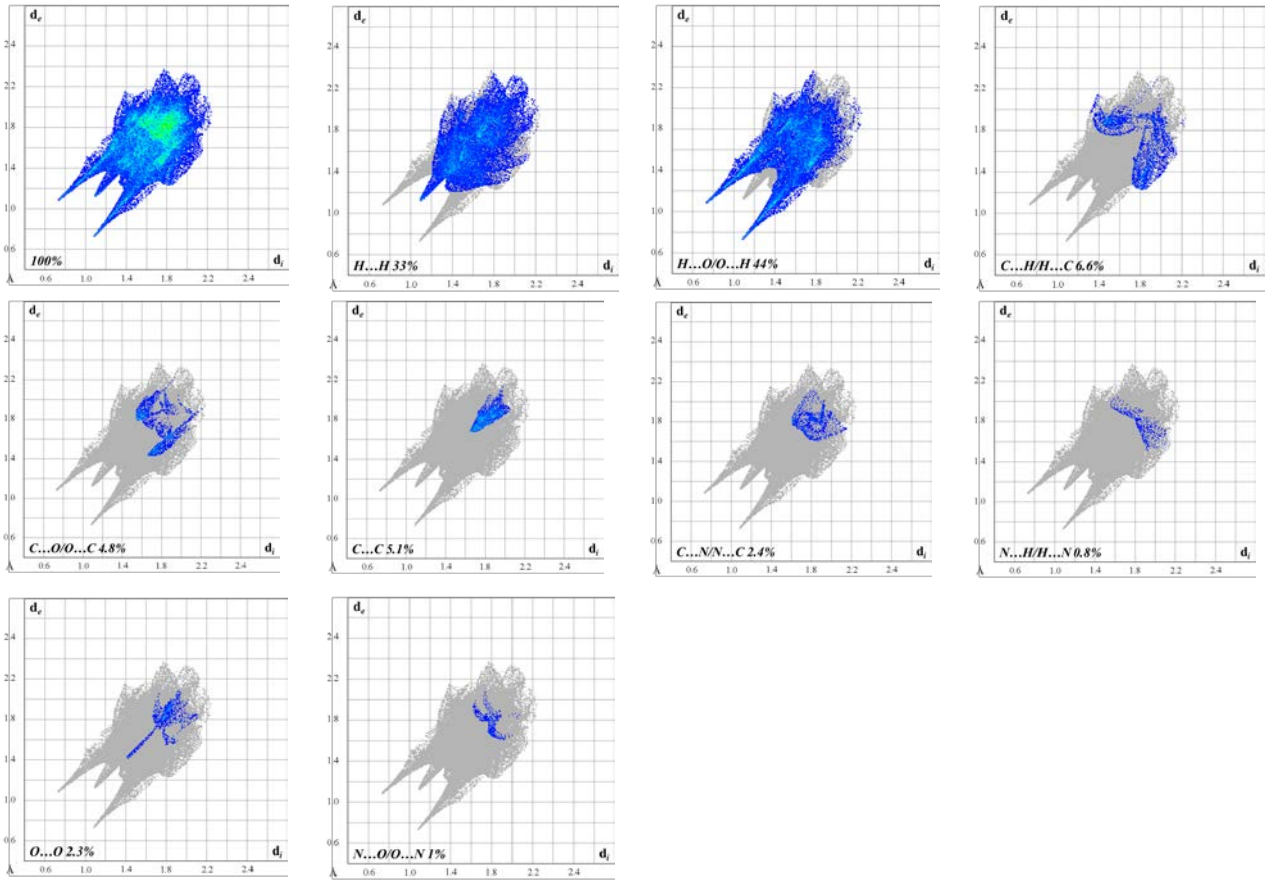

Figure S11. 2D finger print plots of the methanol layer (H_2pOx·MeOH) of $3H_2$pOx·2MeOH·4W.

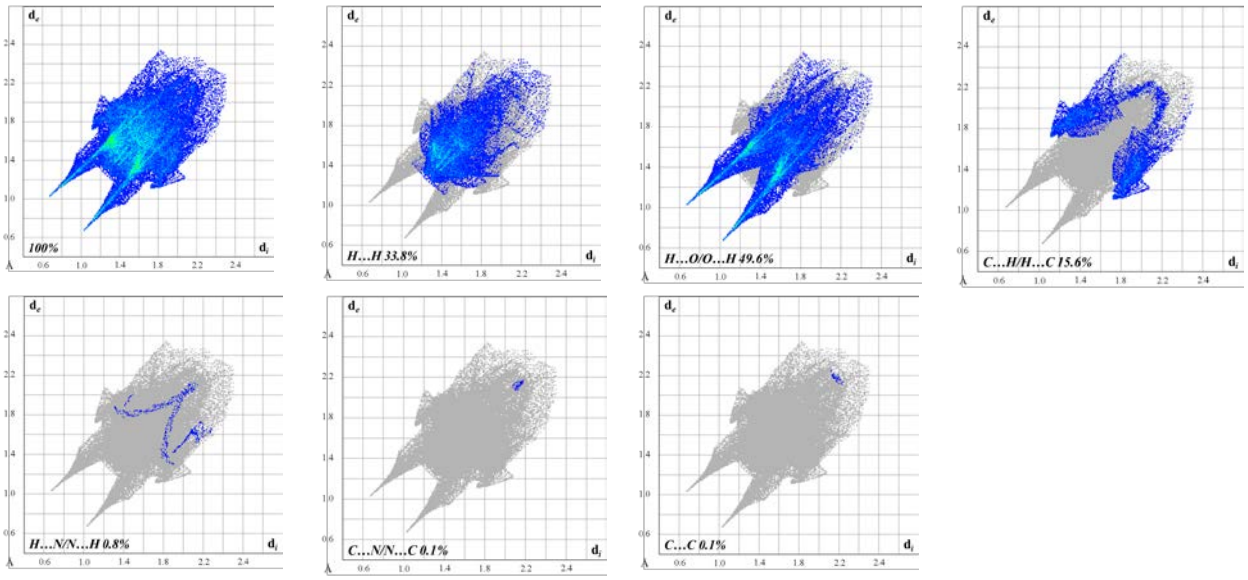

Figure S12. 2D finger print plots of $(HDMA)_2$pOx.

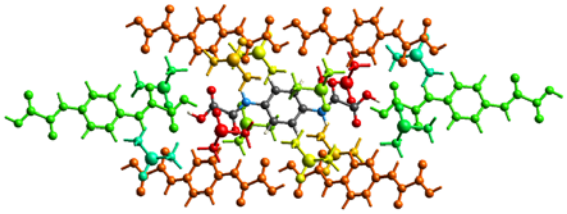

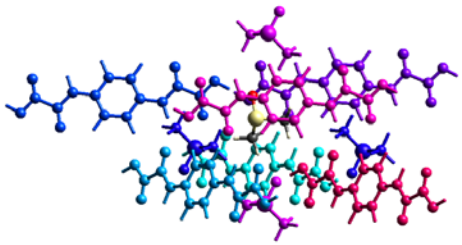

	N	Symop	R	Electron Density	E_ele	E_pol	E_dis	E_rep	E_tot
	2	-	6.25	B3LYP/6-31G(d,p)	-19.0	-4.6	-16.9	17.7	-27.3
	4	-x, y+1/2, -z+1/2	7.91	B3LYP/6-31G(d,p)	-25.5	-6.2	-18.5	29.5	-29.4
	2	-	6.32	B3LYP/6-31G(d,p)	-0.3	-0.8	-10.9	4.1	-7.8
	2	-	5.61	B3LYP/6-31G(d,p)	-0.9	-0.6	-8.2	3.4	-6.4
	2	-	4.40	B3LYP/6-31G(d,p)	-8.7	-1.7	-20.7	13.5	-20.0
	2	x, y, z	14.11	B3LYP/6-31G(d,p)	1.5	-0.4	-3.2	0.2	-1.4
	2	-	9.07	B3LYP/6-31G(d,p)	-92.2	-21.1	-10.8	100.8	-60.2
	2	-	10.45	B3LYP/6-31G(d,p)	2.1	-1.1	-4.2	3.6	-0.1
	0	-	6.32	B3LYP/6-31G(d,p)	-0.3	-0.8	-10.9	4.1	-7.8
	0	-	5.61	B3LYP/6-31G(d,p)	-0.9	-0.6	-8.2	3.4	-6.4
	0	-	9.07	B3LYP/6-31G(d,p)	-92.2	-21.1	-10.8	100.8	-60.2
	0	-x, y+1/2, -z+1/2	6.59	B3LYP/6-31G(d,p)	-1.1	-0.5	-4.9	3.1	-3.9
	0	-	6.25	B3LYP/6-31G(d,p)	-19.0	-4.6	-16.9	17.7	-27.3
	0	x, -y+1/2, z+1/2	5.28	B3LYP/6-31G(d,p)	-15.4	-4.7	-7.6	10.4	-20.0
	0	-	4.40	B3LYP/6-31G(d,p)	-8.7	-1.7	-20.7	13.5	-20.0
	0	-	10.45	B3LYP/6-31G(d,p)	2.1	-1.1	-4.2	3.6	-0.1

	N	Symop	R	Electron Density	E_ele	E_pol	E_dis	E_rep	E_tot
	0	-	6.25	B3LYP/6-31G(d,p)	-19.0	-4.6	-16.9	17.7	-27.3
	0	-x, y+1/2, -z+1/2	7.91	B3LYP/6-31G(d,p)	-25.5	-6.2	-18.5	29.5	-29.4
	0	-	6.32	B3LYP/6-31G(d,p)	-0.3	-0.8	-10.9	4.1	-7.8
	0	-	5.61	B3LYP/6-31G(d,p)	-0.9	-0.6	-8.2	3.4	-6.4
	0	-	4.40	B3LYP/6-31G(d,p)	-8.7	-1.7	-20.7	13.5	-20.0
	0	x, y, z	14.11	B3LYP/6-31G(d,p)	1.5	-0.4	-3.2	0.2	-1.4
	0	-	9.07	B3LYP/6-31G(d,p)	-92.2	-21.1	-10.8	100.8	-60.2
	0	-	10.45	B3LYP/6-31G(d,p)	2.1	-1.1	-4.2	3.6	-0.1
	1	-	6.32	B3LYP/6-31G(d,p)	-0.3	-0.8	-10.9	4.1	-7.8
	1	-	5.61	B3LYP/6-31G(d,p)	-0.9	-0.6	-8.2	3.4	-6.4
	1	-	9.07	B3LYP/6-31G(d,p)	-92.2	-21.1	-10.8	100.8	-60.2
	2	-x, y+1/2, -z+1/2	6.59	B3LYP/6-31G(d,p)	-1.1	-0.5	-4.9	3.1	-3.9
	1	-	6.25	B3LYP/6-31G(d,p)	-19.0	-4.6	-16.9	17.7	-27.3
	2	x, -y+1/2, z+1/2	5.28	B3LYP/6-31G(d,p)	-15.4	-4.7	-7.6	10.4	-20.0
	1	-	4.40	B3LYP/6-31G(d,p)	-8.7	-1.7	-20.7	13.5	-20.0
	1	-	10.45	B3LYP/6-31G(d,p)	2.1	-1.1	-4.2	3.6	-0.1

Figure S13. Environments about the H_2pOx and DMSO in H_2pOx·2DMSO.

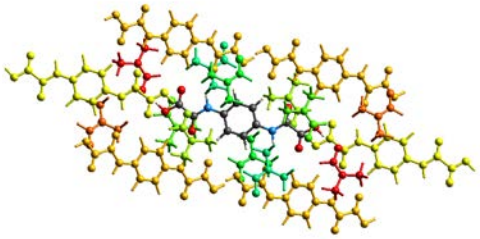

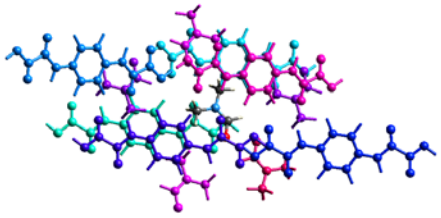

	N	Symop	R	Electron Density	E_ele	E_pol	E_dis	E_rep	E_tot
	2	-	9.35	B3LYP/6-31G(d,p)	-93.5	-22.0	-10.9	109.4	-57.0
	2	-	11.50	B3LYP/6-31G(d,p)	2.9	-0.5	-1.9	0.3	1.3
	4	-x, y+1/2, -z+1/2	8.39	B3LYP/6-31G(d,p)	-25.4	-6.1	-17.9	29.2	-28.9
	2	x, y, z	12.96	B3LYP/6-31G(d,p)	6.0	-1.2	-8.1	2.3	-0.2
	2	-	5.44	B3LYP/6-31G(d,p)	-10.5	-3.3	-17.6	9.1	-23.2
	2	-	6.32	B3LYP/6-31G(d,p)	-7.0	-2.3	-19.0	9.0	-20.1
	2	-	4.69	B3LYP/6-31G(d,p)	-2.7	-1.1	-16.6	6.4	-14.2
	2	-	6.22	B3LYP/6-31G(d,p)	-1.0	-1.0	-12.2	7.7	-7.6
	0	-	6.32	B3LYP/6-31G(d,p)	-7.0	-2.3	-19.0	9.0	-20.1
	0	-	6.22	B3LYP/6-31G(d,p)	-1.0	-1.0	-12.2	7.7	-7.6
	0	-	11.50	B3LYP/6-31G(d,p)	2.9	-0.5	-1.9	0.3	1.3
	0	-	9.35	B3LYP/6-31G(d,p)	-93.5	-22.0	-10.9	109.4	-57.0
	0	-	5.44	B3LYP/6-31G(d,p)	-10.5	-3.3	-17.6	9.1	-23.2
	0	-x, y+1/2, -z+1/2	6.92	B3LYP/6-31G(d,p)	-0.2	-0.3	-2.1	0.2	-2.1
	0	x, -y+1/2, z+1/2	5.70	B3LYP/6-31G(d,p)	-6.9	-2.8	-8.8	10.4	-10.7
	0	-	4.69	B3LYP/6-31G(d,p)	-2.7	-1.1	-16.6	6.4	-14.2
	0	-x, -y, -z	6.06	B3LYP/6-31G(d,p)	-5.1	-0.9	-2.1	0.1	-7.8

	N	Symop	R	Electron Density	E_ele	E_pol	E_dis	E_rep	E_tot
	0	-	9.35	B3LYP/6-31G(d,p)	-93.5	-22.0	-10.9	109.4	-57.0
	0	-	11.50	B3LYP/6-31G(d,p)	2.9	-0.5	-1.9	0.3	1.3
	0	-x, y+1/2, -z+1/2	8.39	B3LYP/6-31G(d,p)	-25.4	-6.1	-17.9	29.2	-28.9
	0	x, y, z	12.96	B3LYP/6-31G(d,p)	6.0	-1.2	-8.1	2.3	-0.2
	0	-	5.44	B3LYP/6-31G(d,p)	-10.5	-3.3	-17.6	9.1	-23.2
	0	-	6.32	B3LYP/6-31G(d,p)	-7.0	-2.3	-19.0	9.0	-20.1
	0	-	4.69	B3LYP/6-31G(d,p)	-2.7	-1.1	-16.6	6.4	-14.2
	0	-	6.22	B3LYP/6-31G(d,p)	-1.0	-1.0	-12.2	7.7	-7.6
	1	-	6.32	B3LYP/6-31G(d,p)	-7.0	-2.3	-19.0	9.0	-20.1
	1	-	6.22	B3LYP/6-31G(d,p)	-1.0	-1.0	-12.2	7.7	-7.6
	1	-	11.50	B3LYP/6-31G(d,p)	2.9	-0.5	-1.9	0.3	1.3
	1	-	9.35	B3LYP/6-31G(d,p)	-93.5	-22.0	-10.9	109.4	-57.0
	1	-	5.44	B3LYP/6-31G(d,p)	-10.5	-3.3	-17.6	9.1	-23.2
	2	-x, y+1/2, -z+1/2	6.92	B3LYP/6-31G(d,p)	-0.2	-0.3	-2.1	0.2	-2.1
	2	x, -y+1/2, z+1/2	5.70	B3LYP/6-31G(d,p)	-6.9	-2.8	-8.8	10.4	-10.7
	1	-	4.69	B3LYP/6-31G(d,p)	-2.7	-1.1	-16.6	6.4	-14.2
	1	-x, -y, -z	6.06	B3LYP/6-31G(d,p)	-5.1	-0.9	-2.1	0.1	-7.8

Figure S14. Environments about the H_2pOx and 2DMF in H_2pOx·2DMF.

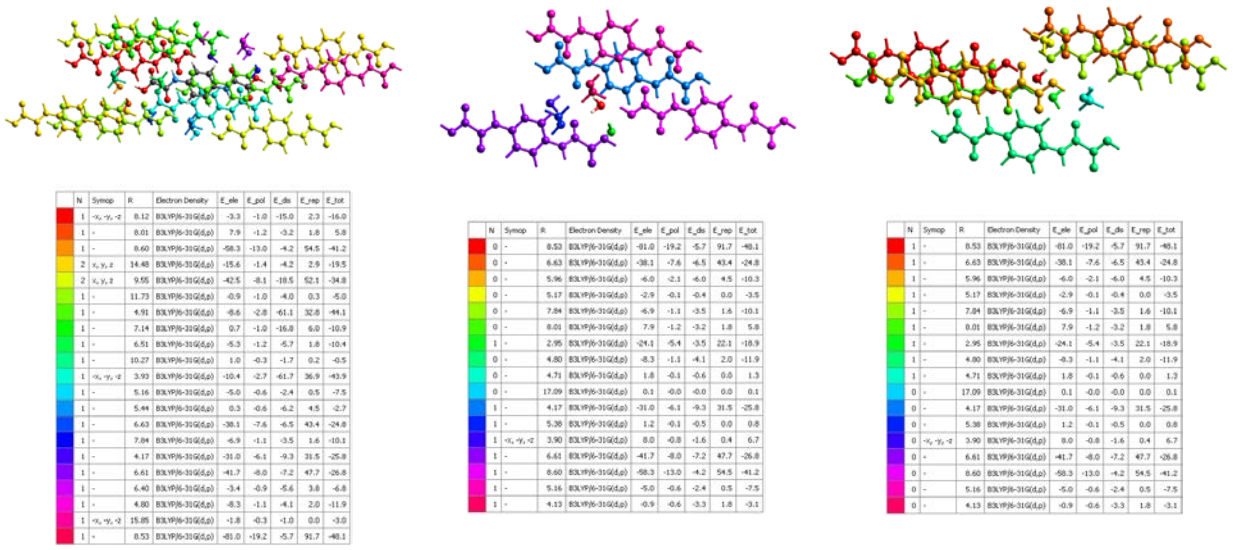

	N	Symop	R	Electron Density	E_ele	E_pol	E_dis	E_rep	E_tot
	1	-x, -y, -z	8.12	B3LYP/6-31G(d,p)	-3.3	-1.0	-15.0	2.3	-16.0
	1	-	8.01	B3LYP/6-31G(d,p)	7.9	-1.2	-3.2	1.8	5.8
	1	-	8.60	B3LYP/6-31G(d,p)	-58.3	-13.0	-4.2	54.5	-41.2
	2	x, y, z	14.48	B3LYP/6-31G(d,p)	-15.6	-1.4	-4.2	2.9	-19.5
	2	x, y, z	9.55	B3LYP/6-31G(d,p)	-42.5	-8.1	-10.5	52.1	-34.8
	1	-	11.73	B3LYP/6-31G(d,p)	-0.9	-1.0	-4.0	0.3	-5.0
	1	-	4.91	B3LYP/6-31G(d,p)	-8.6	-2.8	-61.1	32.8	-44.1
	1	-	7.14	B3LYP/6-31G(d,p)	0.7	-1.0	-16.8	6.0	-10.9
	1	-	6.51	B3LYP/6-31G(d,p)	-5.3	-1.2	-5.7	1.8	-10.4
	1	-	10.27	B3LYP/6-31G(d,p)	1.0	-0.3	-1.7	0.2	-0.5
	1	-x, -y, -z	3.93	B3LYP/6-31G(d,p)	-10.4	-2.7	-61.7	36.9	-43.9
	1	-	5.16	B3LYP/6-31G(d,p)	-5.0	-0.6	-2.4	0.5	-7.5
	1	-	5.44	B3LYP/6-31G(d,p)	0.3	-0.6	-6.2	4.5	-2.7
	1	-	6.63	B3LYP/6-31G(d,p)	-38.1	-7.6	-6.5	43.4	-24.8
	1	-	7.84	B3LYP/6-31G(d,p)	-6.9	-1.1	-3.5	1.6	-10.1
	1	-	4.17	B3LYP/6-31G(d,p)	-31.0	-6.1	-9.3	31.5	-25.8
	1	-	6.61	B3LYP/6-31G(d,p)	-41.7	-8.0	-7.2	47.7	-26.8
	1	-	6.40	B3LYP/6-31G(d,p)	-3.4	-0.9	-5.6	3.8	-6.8
	1	-	4.80	B3LYP/6-31G(d,p)	-8.3	-1.1	-4.1	2.0	-11.9
	1	-x, -y, -z	15.85	B3LYP/6-31G(d,p)	-1.8	-0.3	-1.0	0.0	-3.0
	1	-	8.53	B3LYP/6-31G(d,p)	-81.0	-19.2	-5.7	91.7	-48.1

	N	Symop	R	Electron Density	E_ele	E_pol	E_dis	E_rep	E_tot
	0	-	8.53	B3LYP/6-31G(d,p)	-81.0	-19.2	-5.7	91.7	-48.1
	0	-	6.63	B3LYP/6-31G(d,p)	-38.1	-7.6	-6.5	43.4	-24.8
	0	-	5.96	B3LYP/6-31G(d,p)	-6.0	-2.1	-6.0	4.5	-10.3
	0	-	5.17	B3LYP/6-31G(d,p)	-2.9	-0.1	-0.4	0.0	-3.5
	0	-	7.84	B3LYP/6-31G(d,p)	-6.9	-1.1	-3.5	1.6	-10.1
	0	-	8.01	B3LYP/6-31G(d,p)	7.9	-1.2	-3.2	1.8	5.8
	1	-	2.95	B3LYP/6-31G(d,p)	-24.1	-5.4	-3.5	22.1	-10.9
	0	-	4.80	B3LYP/6-31G(d,p)	-8.3	-1.1	-4.1	2.0	-11.9
	0	-	4.71	B3LYP/6-31G(d,p)	1.8	-0.1	-0.6	0.0	1.3
	0	-	17.09	B3LYP/6-31G(d,p)	0.1	-0.0	-0.0	0.0	0.1
	1	-	4.17	B3LYP/6-31G(d,p)	-31.0	-6.1	-9.3	31.5	-25.8
	1	-	5.38	B3LYP/6-31G(d,p)	1.2	-0.1	-0.5	0.0	0.8
	1	-x, -y, -z	3.90	B3LYP/6-31G(d,p)	8.0	-0.8	-1.6	0.4	6.7
	1	-	6.61	B3LYP/6-31G(d,p)	-41.7	-8.0	-7.2	47.7	-26.8
	1	-	8.60	B3LYP/6-31G(d,p)	-58.3	-13.0	-4.2	54.5	-41.2
	1	-	5.16	B3LYP/6-31G(d,p)	-5.0	-0.6	-2.4	0.5	-7.5
	1	-	4.13	B3LYP/6-31G(d,p)	-0.9	-0.6	-3.3	1.8	-3.1

	N	Symop	R	Electron Density	E_ele	E_pol	E_dis	E_rep	E_tot
	1	-	8.53	B3LYP/6-31G(d,p)	-81.0	-19.2	-5.7	91.7	-48.1
	1	-	6.63	B3LYP/6-31G(d,p)	-38.1	-7.6	-6.5	43.4	-24.8
	1	-	5.96	B3LYP/6-31G(d,p)	-6.0	-2.1	-6.0	4.5	-10.3
	1	-	5.17	B3LYP/6-31G(d,p)	-2.9	-0.1	-0.4	0.0	-3.5
	1	-	7.84	B3LYP/6-31G(d,p)	-6.9	-1.1	-3.5	1.6	-10.1
	1	-	8.01	B3LYP/6-31G(d,p)	7.9	-1.2	-3.2	1.8	5.8
	1	-	2.95	B3LYP/6-31G(d,p)	-24.1	-5.4	-3.5	22.1	-10.9
	1	-	4.80	B3LYP/6-31G(d,p)	-8.3	-1.1	-4.1	2.0	-11.9
	1	-	4.71	B3LYP/6-31G(d,p)	1.8	-0.1	-0.6	0.0	1.3
	0	-	17.09	B3LYP/6-31G(d,p)	0.1	-0.0	-0.0	0.0	0.1
	0	-	4.17	B3LYP/6-31G(d,p)	-31.0	-6.1	-9.3	31.5	-25.8
	0	-	5.38	B3LYP/6-31G(d,p)	1.2	-0.1	-0.5	0.0	0.8
	0	-x, -y, -z	3.90	B3LYP/6-31G(d,p)	8.0	-0.8	-1.6	0.4	6.7
	0	-	6.61	B3LYP/6-31G(d,p)	-41.7	-8.0	-7.2	47.7	-26.8
	0	-	8.60	B3LYP/6-31G(d,p)	-58.3	-13.0	-4.2	54.5	-41.2
	0	-	5.16	B3LYP/6-31G(d,p)	-5.0	-0.6	-2.4	0.5	-7.5
	0	-	4.13	B3LYP/6-31G(d,p)	-0.9	-0.6	-3.3	1.8	-3.1

Figure S15. Environments about the H_2pOx and water molecules in 3H_2pOx·2MeOH·4W.

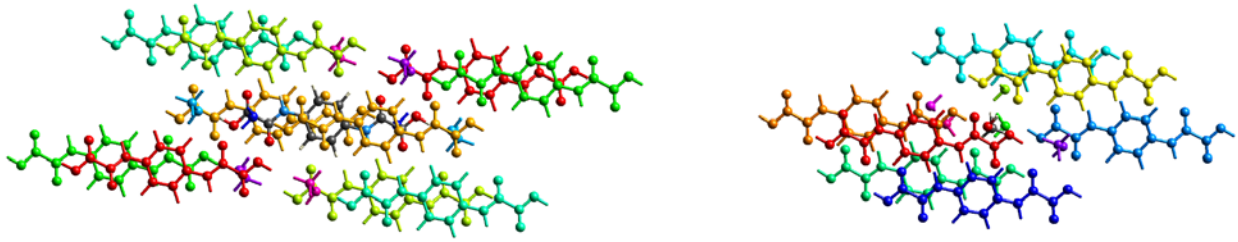

	N	Symop	R	Electron Density	E_ele	E_pol	E_dis	E_rep	E_tot
	2	-	11.73	B3LYP/6-31G(d,p)	-0.9	-1.0	-4.0	0.3	-5.0
	2	-	4.91	B3LYP/6-31G(d,p)	-8.6	-2.8	-61.1	32.8	-44.1
	2	-	7.14	B3LYP/6-31G(d,p)	0.7	-1.0	-16.8	6.0	-10.9
	2	x, y, z	14.48	B3LYP/6-31G(d,p)	-16.7	-1.5	-4.6	4.0	-20.4
	2	x, y, z	9.55	B3LYP/6-31G(d,p)	-38.5	-7.1	-17.9	43.1	-35.0
	2	-	8.78	B3LYP/6-31G(d,p)	-77.1	-19.8	-8.8	90.9	-47.6
	2	-	5.96	B3LYP/6-31G(d,p)	-6.0	-2.1	-6.0	4.5	-10.3
	2	-	6.55	B3LYP/6-31G(d,p)	-37.7	-8.2	-10.5	45.5	-27.0
	2	-	4.72	B3LYP/6-31G(d,p)	-7.5	-1.4	-10.0	5.9	-14.0

	N	Symop	R	Electron Density	E_ele	E_pol	E_dis	E_rep	E_tot
	1	-	6.51	B3LYP/6-31G(d,p)	-5.3	-1.2	-5.7	1.8	-10.4
	1	-	8.78	B3LYP/6-31G(d,p)	-77.1	-19.8	-8.8	90.9	-47.6
	1	-	6.55	B3LYP/6-31G(d,p)	-37.7	-8.2	-10.5	45.5	-27.0
	1	-	5.17	B3LYP/6-31G(d,p)	-2.9	-0.1	-0.4	0.0	-3.5
	1	-	4.13	B3LYP/6-31G(d,p)	-0.9	-0.6	-3.3	1.8	-3.1
	1	-	6.40	B3LYP/6-31G(d,p)	-3.4	-0.9	-5.6	3.8	-6.8
	1	-	5.44	B3LYP/6-31G(d,p)	0.3	-0.6	-6.2	4.5	-2.7
	1	-	10.27	B3LYP/6-31G(d,p)	1.0	-0.3	-1.7	0.2	-0.5
	1	-	4.72	B3LYP/6-31G(d,p)	-7.5	-1.4	-10.0	5.9	-14.0
	1	-x, -y, -z	4.94	B3LYP/6-31G(d,p)	-0.5	-0.1	-1.2	0.1	-1.6
	1	-	4.71	B3LYP/6-31G(d,p)	1.8	-0.1	-0.6	0.0	1.3
	1	-	5.38	B3LYP/6-31G(d,p)	1.2	-0.1	-0.5	0.0	0.8

Figure S16. Environments about the H_2pOx and MeOH molecules in 3H_2pOx·2MeOH·4W.

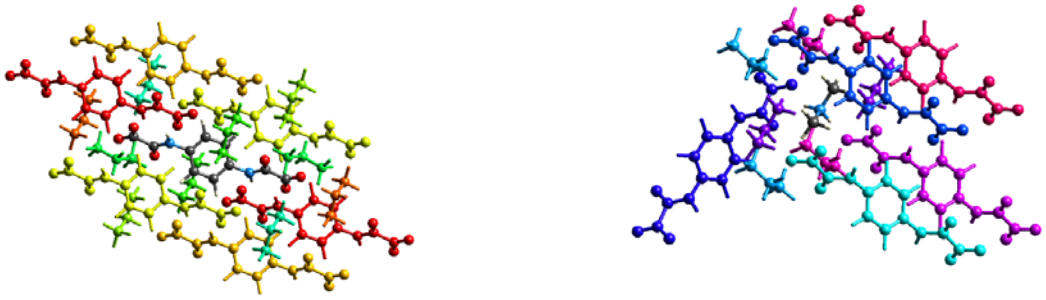

	N	Symop	R	Electron Density	E_ele	E_pol	E_dis	E_rep	E_tot
	2	x, y, z	9.20	B3LYP/6-31G(d,p)	-53.2	-12.2	-15.6	54.8	-45.0
	2	-	8.70	B3LYP/6-31G(d,p)	-91.4	-6.0	-12.2	222.9	26.1
	2	x, y, z	7.00	B3LYP/6-31G(d,p)	9.1	-6.3	-17.4	7.4	-5.6
	2	x, y, z	5.97	B3LYP/6-31G(d,p)	12.0	-5.7	-23.2	8.4	-6.6
	2	-	6.63	B3LYP/6-31G(d,p)	-2.2	-1.8	-9.8	9.2	-6.5
	2	-	4.02	B3LYP/6-31G(d,p)	-4.6	-2.3	-23.0	25.9	-10.7
	2	-	7.09	B3LYP/6-31G(d,p)	-61.7	-4.8	-14.8	176.4	27.4
	2	-	6.92	B3LYP/6-31G(d,p)	-1.4	-1.5	-9.5	4.7	-7.9
	0	-	6.92	B3LYP/6-31G(d,p)	-1.4	-1.5	-9.5	4.7	-7.9
	0	-x+1/2, y+1/2, -z+1/2	5.19	B3LYP/6-31G(d,p)	-2.5	-0.2	-5.7	9.2	-2.0
	0	-	4.02	B3LYP/6-31G(d,p)	-4.8	-2.7	-23.0	26.0	-11.1
	0	-	7.09	B3LYP/6-31G(d,p)	-61.7	-4.8	-14.8	176.4	27.4
	0	x, y, z	5.97	B3LYP/6-31G(d,p)	-0.3	-0.1	-2.6	1.4	-1.7
	0	-	8.70	B3LYP/6-31G(d,p)	-91.4	-6.0	-12.2	222.9	26.1
	0	-x+1/2, y+1/2, -z+1/2	5.38	B3LYP/6-31G(d,p)	-0.6	-0.2	-3.7	10.2	2.3
	0	-	6.63	B3LYP/6-31G(d,p)	-2.2	-1.8	-9.8	9.2	-6.5

	N	Symop	R	Electron Density	E_ele	E_pol	E_dis	E_rep	E_tot
	0	x, y, z	9.20	B3LYP/6-31G(d,p)	-53.2	-12.2	-15.6	54.8	-45.0
	0	-	8.70	B3LYP/6-31G(d,p)	-91.4	-6.0	-12.2	222.9	26.1
	0	x, y, z	7.00	B3LYP/6-31G(d,p)	9.1	-6.3	-17.4	7.4	-5.6
	0	x, y, z	5.97	B3LYP/6-31G(d,p)	12.0	-5.7	-23.2	8.4	-6.6
	0	-	6.63	B3LYP/6-31G(d,p)	-2.2	-1.8	-9.8	9.2	-6.5
	0	-	4.02	B3LYP/6-31G(d,p)	-4.6	-2.3	-23.0	25.9	-10.7
	0	-	7.09	B3LYP/6-31G(d,p)	-61.7	-4.8	-14.8	176.4	27.4
	0	-	6.92	B3LYP/6-31G(d,p)	-1.4	-1.5	-9.5	4.7	-7.9
	1	-	6.92	B3LYP/6-31G(d,p)	-1.4	-1.5	-9.5	4.7	-7.9
	2	-x+1/2, y+1/2, -z+1/2	5.19	B3LYP/6-31G(d,p)	-2.5	-0.2	-5.7	9.2	-2.0
	1	-	4.02	B3LYP/6-31G(d,p)	-4.8	-2.7	-23.0	26.0	-11.1
	1	-	7.09	B3LYP/6-31G(d,p)	-61.7	-4.8	-14.8	176.4	27.4
	2	x, y, z	5.97	B3LYP/6-31G(d,p)	-0.3	-0.1	-2.6	1.4	-1.7
	1	-	8.70	B3LYP/6-31G(d,p)	-91.4	-6.0	-12.2	222.9	26.1
	2	-x+1/2, y+1/2, -z+1/2	5.38	B3LYP/6-31G(d,p)	-0.6	-0.2	-3.7	10.2	2.3
	1	-	6.63	B3LYP/6-31G(d,p)	-2.2	-1.8	-9.8	9.2	-6.5

Figure S17. Environments about the H_2pOx and $HDMA^+$ ions in $(HDMA)_2pOx$.

Table S10. Interaction (E_{m-m}) and lattice energies (E_L) in kJmol^{-1} of $H_2pOx{\cdot}2S$ calculated with the CLP-PIXEL software. H_2pOx (m = 1) and S (m = 2) are the interacting fragments.

$H_2pOx{\cdot}2S$	E_{1-1}	E_{1-2}	E_{2-2}	E_L[a]	Torsion-angle (φ, °)
$H_2pOx{\cdot}2DMSO$	-149.9	-44.8	-15.0	-134.8	-11.7(3)
$H_2pOx{\cdot}2DMF$	-139.1	-94.7	-9.8	-174.1	2.84(19)
$3H_2pOx{\cdot}2MeOH{\cdot}4W$				-216.7[b]	
$H_2pOx{\cdot}2W1$	-185.1	-50.8	-4.2	-147.6	21.2(4)
$H_2pOx{\cdot}2W2$	-185.2	-63.7	1.7	-154.6	3.8(4)
$H_2pOx{\cdot}2MeOH$	-185.0	-34.5	-4.3	-131.3	8.2(4)

[a] E_L was calculated as $E_L = (E_{1-1} + n*E_{2-2})/2 + E_{1-2}$, where n = number of solvent molecules. [b] Calculated as $E_{L\text{-}2MeOH\cdot4W} = ½ (E_{L\text{-}W1} + E_{L\text{-}W2} + E_{L\text{-}MeOH})$

6. Thermal analysis

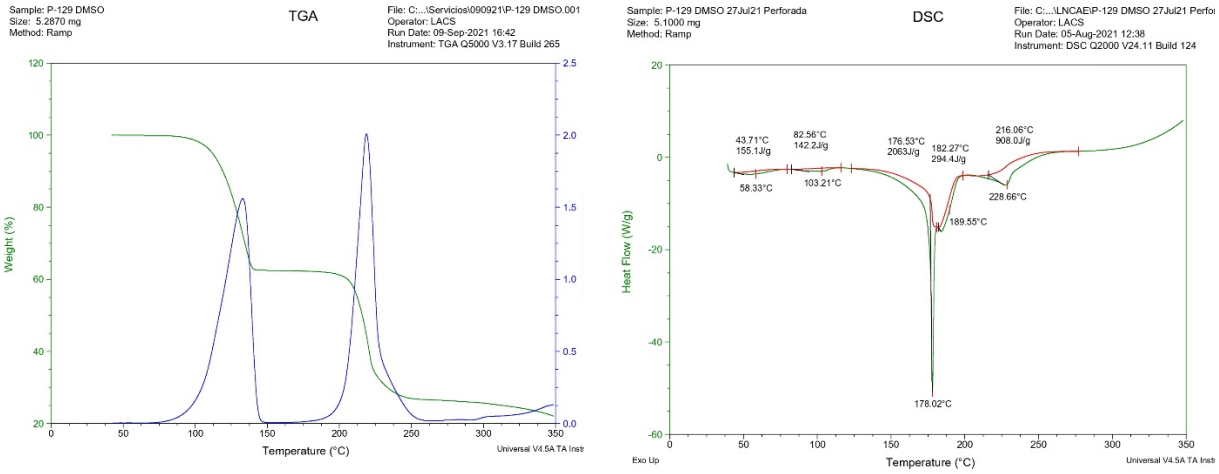

Figure S18. TG and DSC recordings of H_2pOx·2DMSO.

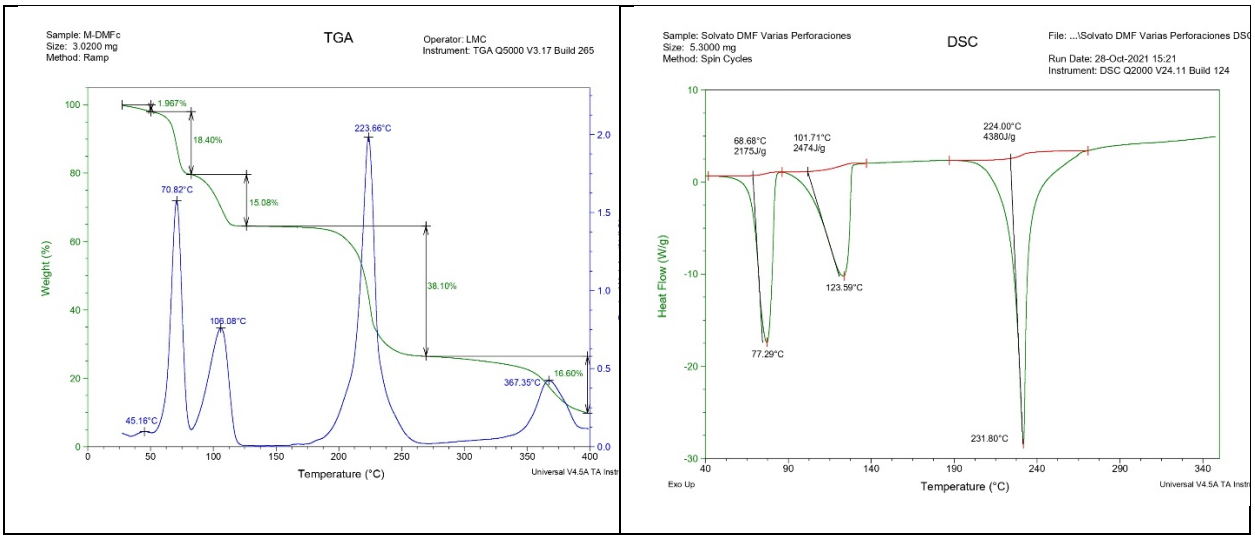

Figure S19. TG and DSC recordings of powdered H_2pOx·2DMF.

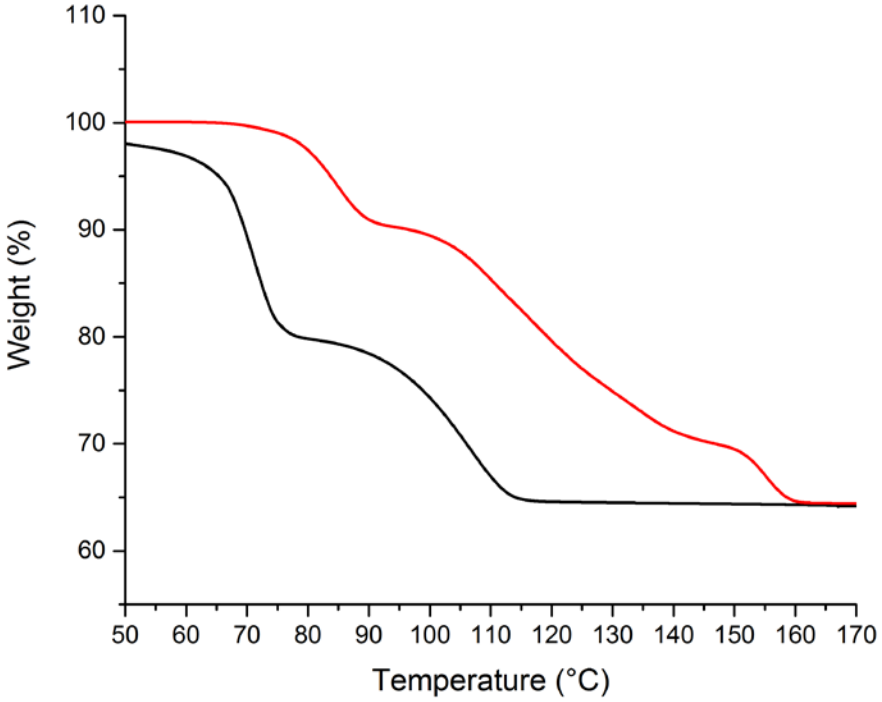

Figure S20. TG recordings of powdered mc-H_2pOx·2DMF (black) and lc-H_2pOx·2DMF (red)

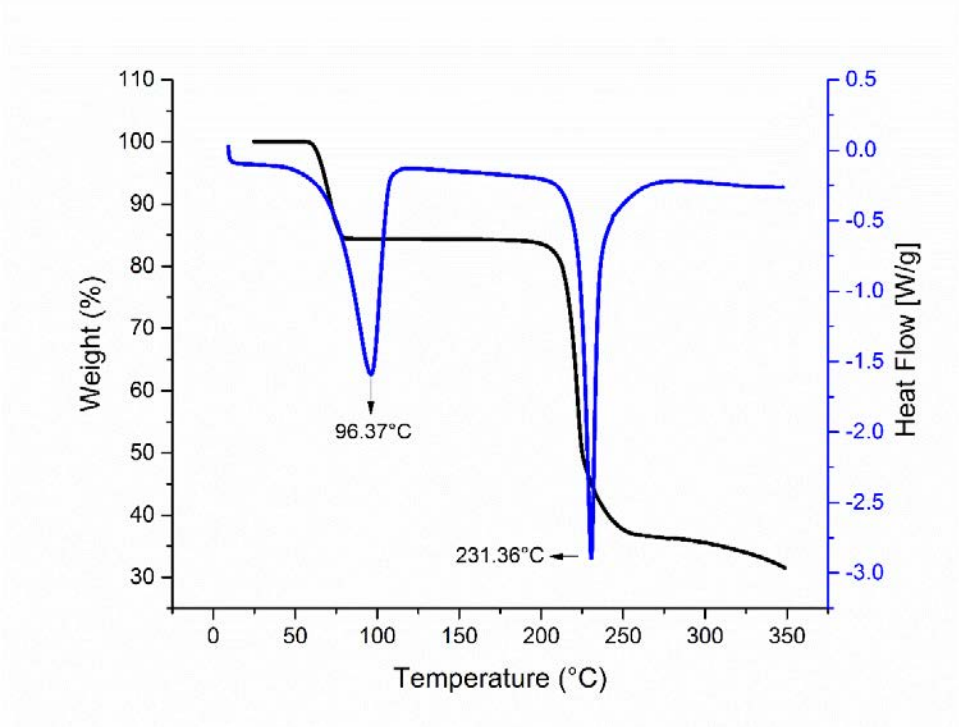

Figure S21. TG and DSC recordings of 3H_2pOx·2MeOH·4W

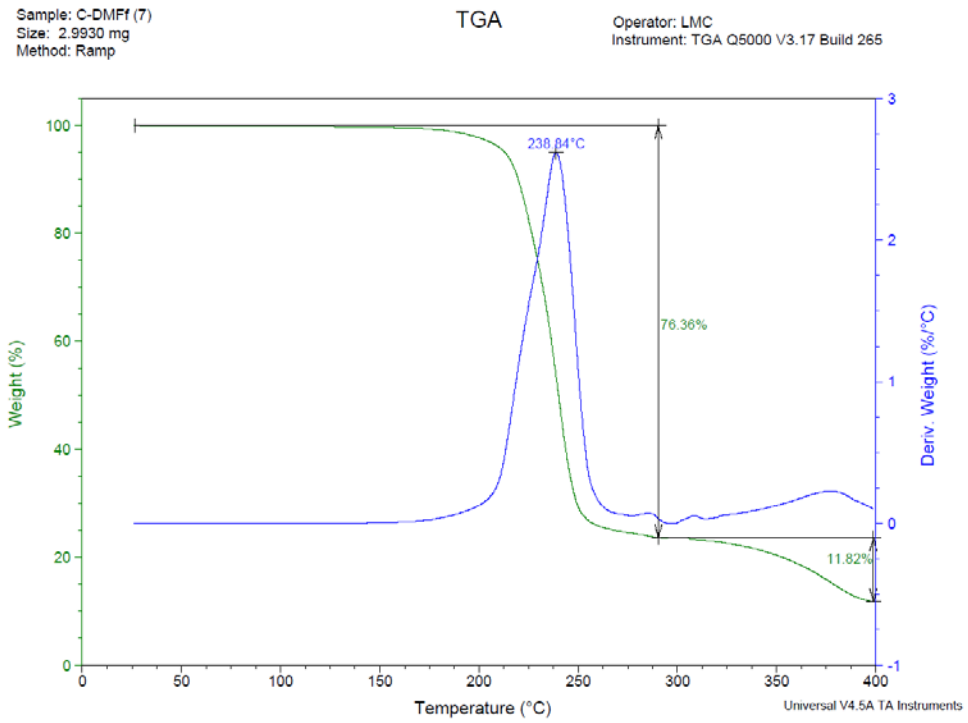

Figure S22. TG and Δw/ΔT recordings of $(HDMA)_2pOx$.

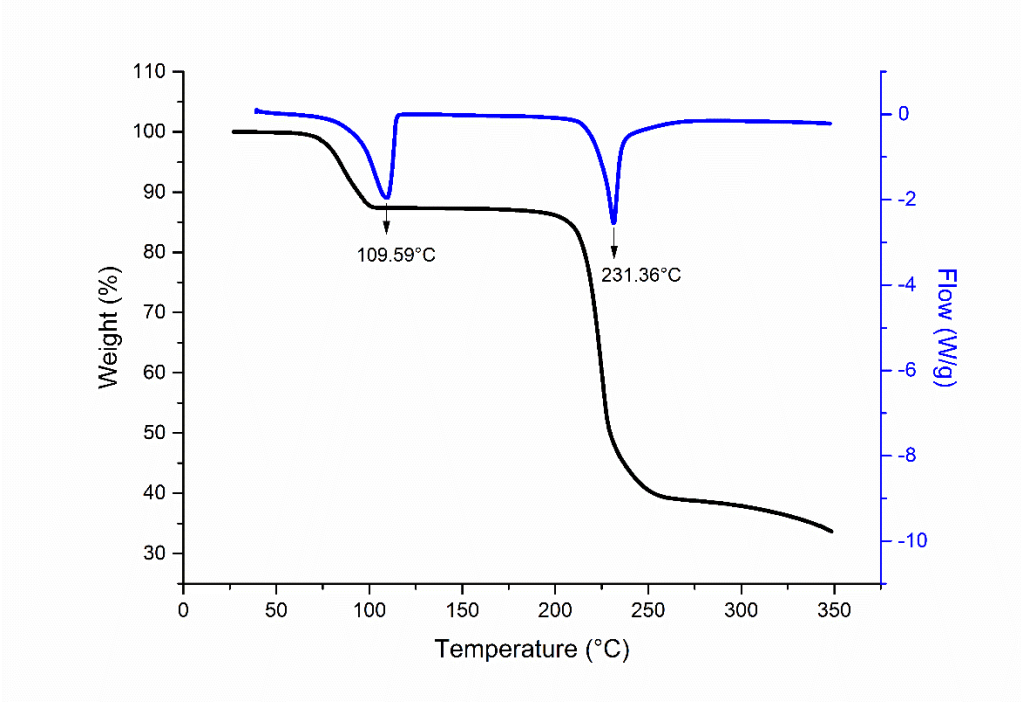

Figure S23. TG and DSC recordings of $H_2pOx{\cdot}2W$ (H-I).

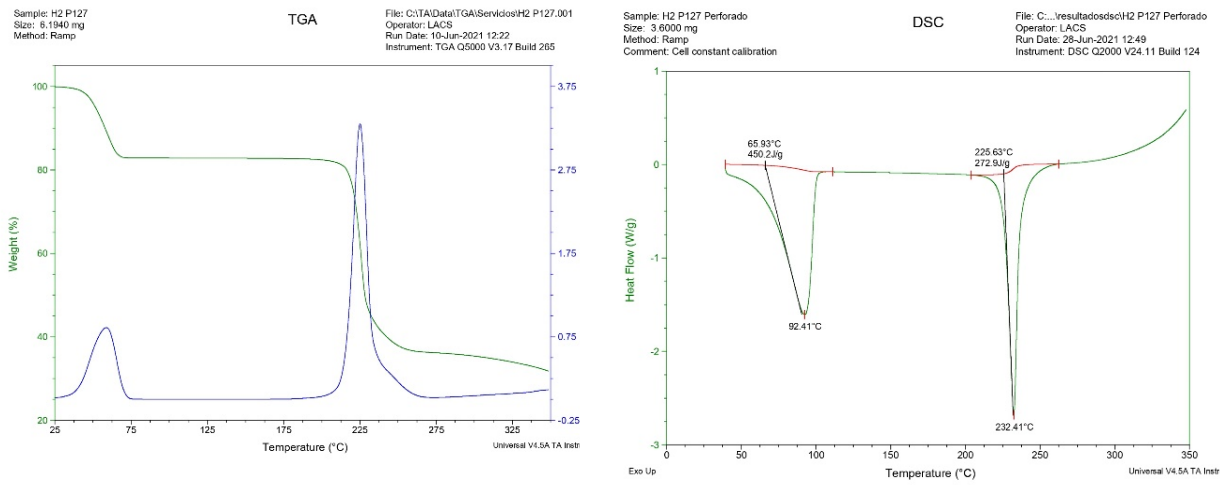

Figure S24. TG (a) and DSC (b) recordings of H_2pOx·2W (H-II).

Table S11. TG and DSC data of H_2pOx solvates, desolvates and HDMA salt.

Compound	Theor./Exp. step stoichiometry (%)	Peak temperature DSC, (°C)[a]	Observations
H_2pOx·2DMSO	38.2/38.0	178.0	2 Crystallyzed DMSO molecules
		228.7	Decomposition
mc-H_2pOx·2DMF powdered crystals	36.7/33.5 (18.4, 15.1)	77.3, 126.6	2 Crystallyzed DMF molecules
		232.1	Decomposition
Lc-H_2pOx·2DMF Large crystals	36.7/35.6 (9.5, 20.2, 5.9)	95.8, 123.0, 159.0	2 Crystallyzed DMF molecules
		228.9	Decomposition
$3H_2$pOx·2MeOH·4W	15.3/15.3	96.4	Single loss of 2 MeOH and 4 W *per* $3H_2$POx molecules
		231.4	Decomposition
$(HDMA)_2$pOx·		238.8	Decomposition
H-I	12.5/12.6	109.6	2 Water molecules
		231.4	Decomposition
H-II	12.5/12.7	92.4	2 Water molecules
		232.4	Decomposition

ΔH_v /kJ mol^{-1}: 52.1 (DMSO), 49.2 (DMF), 37.0 (MeOH, 40.656 (W) [18]

7. Vibrational spectroscopy data.

Table S12. Stretching IR absorptions of microcrystalline powders of $H_2pOx{\cdot}2$ (S = DMSO, DMF, ⅓(2MeOH·2W), W = water), H_2pOx (desolvates) and reported values for oxalic acid ($H_2C_2O_4$)[19,20].

	Bond wavenumbers (cm^{-1})					
	O—H (W)	O—H	N—H	$C{=}O_{as}$	$C{=}O_{s}$	Fingerprint region
$H_2pOx{\cdot}2DMSO$[a]		3323 (m)	3323 (m)	1706 (sh)	1679 (vs)	1291 (s), 1187 (s)
$H_2pOx{\cdot}2DMF$[b]		3313 (m)	3313 (m)	1730 (w)	1686 (vs)	1295 (m), 1180 (s)
$3H_2pOx{\cdot}2MeOH{\cdot}4W$	3494 (b)	3320 (b)	3310 (m)	1732 (w), 1709 (sh)	1668 (s), 1654 (s)	1244 (s,b), 1190 (s,b)
$(HDMA)_2pOx$			3252 (m) 2684, 2472 ($^+NH_2Me_2$) 1630 (m, b, bending)	1671 (m)	1652 (w)	1395 (s), 1346 (s, b) 1228 (s), 1196 (s)
H-I	3488 (b)	3349 (b)	3335 (m) 3307 (m)	1733 (m) 1714 (m)	1681 (s) 1657 (s)	1299 (m), 1253 (m), 1019 (m)
H-II	3547 (b)	3389 (b)	3316 (m)	1706 (m)	1659 (s)	1272 (s,b), 1198 (m)
A-I		3233 (m)	3312 (m)	1751 (vs)	1677 (vs)	1367 (s,b), 1311 (m) 1214 (m), 1184 (m)
A-II		3226 (m, b)	3311 (m)	1750 (vs)	1673 (vs)	1370 (s,b), 1307 (b,w) 1225 (sh), 1211 (m), 1182 (m)
A-III		3293 (m)	3293 (m)	1766 (s)	1677 (vs)	1371 (s,b), 1303 (s), 1212 (m), 1173 (m)
α-$H_2C_2O_4$		3285 (sh), 3114 (s), 2931 (sh)		1756 (s), 1722 (sh)	1697 (s)	1176 (s)
β-$H_2C_2O_4$		3106 (m), 3014 (m), 2890 (m), 2677 (m)		1732 (s)	1692 (sh)	1237 (s)
$H_2C_2O_4{\cdot}2W$	3501 (s)	3436 (s)		1738 (R)[c]	1688 (s)	1255 (s), 1133 (m)

[a] $\nu S{=}O$ = 997 (m); [b] $\nu C{=}O$ (DMF) = 1686 (s); [c] Raman.

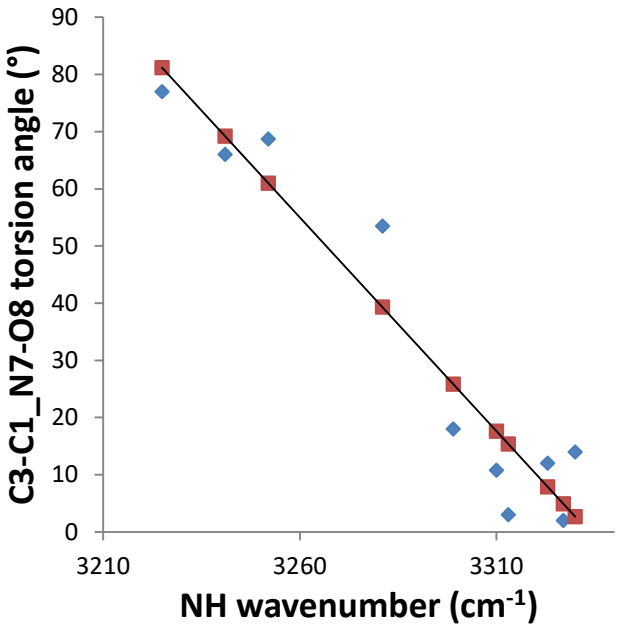

Figure S25. Correlation between the C3—C1—N7—C8 torsion angle and stretching amide NH wavenumber. The data fit to the general equation: C3—C1—N7—C8 torsion angle = 2493(±268) – 0.748(±0.082)ν_{NH} (n = 10, R = 0.956, Sr = 9.4). The data used for correlation are in Table S12.

Table S13. Data used for the correlation of Figure S15 which includes phenyl oxalamates and oxalamides as well as a pair of molecular cocrystals.

Comp.	NH wavenumber (cm^{-1})	C3—C1—N7—C8 torsion angle (°)
$(HDMA)_2pOx$	3252	68.7
2	3241	66
3	3225	77
5	3281	53.5
6	3299	18
1-2b	3330	14
1-2c	3327	2
$H_2pOx·2DMSO$	3323	12
$H_2pOx·2DMF$	3313	3
$3H_2pOx·2MeOH·4W$	3310	10.8

The structures of compounds **2, 3, 5** and **6** are in reference [21] and those of **1-2b** and **1-2c** in reference [22].

8. ^{13}C-CPMAS NMR chemical shifts.

Table S14. ^{13}C-CPMAS NMR chemical shifts of H_2pOx·2S, hydrates I-II and desolvates I-III.

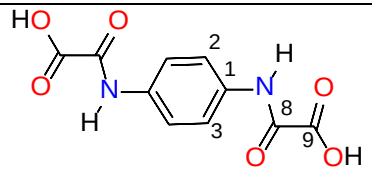

Compound	C1	C2	C3	C8	C9	XCH_3 (X = S, O, N)
H_2pOx (DMSO-d6 solution)	134.6	121.0	121.0	157.1	162.6	39.9
H_2pOx·2DMSO	136	121	123	157	163	37, 33
H_2pOx·2DMF[a]	135	121	121	156, 167 (DMF)	163	37, 32
3H_2pOx·2MeOH·4W	136, 133	122	122	157	162	50
$(HDMA)_2$pOx (D_2O solution)	133.4	121.9	121.9	162.7	165.5	34.1
$(HDMA)_2$pOx	137	130	132	163	164	34, 32
H-I	134, 132	121, 120	124, 121	158, 156	163, 160	
H-II	135	119	122	157	162	
A-I	134	121	121	155	163	
A-II	134	120	121	155	162	
A-III	132, 131	123	124	155, 154	161	

[a] Free DMF: δCO = 162.6, δMe = 36.4, 31.3

7. **References**

(1) CrysAlis PRO, Agilent Technologies: Yarnton, UK, 2012.

(2) G.M. Sheldrick, Crystal structure refinement with SHELXL, *Acta Cryst. C* 2015, **C71**, 3.

(3) L. J. Farrugia, WinGX and ORTEP for windows: An update. *J. Appl. Crystallogr.* 2012, **45**, 849.

(4) A. L. Spek, Structure validation in chemical crystallography, *Acta Crystallogr.* 2009, **D65**, 148.

(5) C. F. Macrae, I. J. Bruno, J. A. Chisholm, P. R. Edgington, P. McCabe, E. Pidcock, V. Rodriguez-Monge, R. Taylor, J. van de Streek, P. A. Wood, Mercury CSD 2.0 - New Features for the Visualization and Investigation of Crystal Structures, *J. Appl. Cryst.* 2008, **41**, 466.

(6) J. Bernstein, R. E. Davis, L. Shimoni, N. L. Chang, Patterns in Hydrogen Bonding: Functionality and Graph Set Analysis in Crystals, *Angew. Chem., Int. Ed. Engl.* 1995, **34**, 1555.

(7) M. A. Spackman, J. J. McKinnon, Fingerprinting intermolecular interactions in molecular crystals, CrystEngComm 2002, **66**, 378.

(8) M. A. Spackman, D. Jayatilaka, Hirshfeld surface analysis, *CrystEngComm* 2009, **11**, 19.

(9) J. J. McKinnon, M. A. Spackman, A. S. Mitchell, Novel tools for visualizing and exploring intermolecular interactions in molecular crystals, Acta Crystallographica B Structural Science 2004, **60**, 627.

(10) M. J. Turner, S. P. Thomas, M. W. Shi, D. Jayatilaka, M. A. Spackman, Energy frameworks: insights into interaction anisotropy and the mechanical properties of molecular crystals. *Chem. Commun.* 2015, **51**, 3735.

(11) C. F. Mackenzie, P. R. Spackman, D. Jayatilaka, M. A. Spackman, CrystalExplorer model energies and energy frameworks: extension to metal coordination compounds, organic salts, solvates and open-shell systems, IUCrJ 2017, **4**, 575.

(12) J. J. McKinnon, D. Jayatilaka, M. A. Spackman, Towards quantitative analysis of intermolecular interactions with Hirshfeld surfaces, Chem. Comm. 2007, **37**, 3814.

(13) M. J. Frisch, G. W. Trucks, H. B. Schlegel, G. E. Scuseria, M. A. Robb, J. R. Cheeseman, G. Scalmani, V. Barone, B. Mennucci, G. A. Petersson, H. Nakatsuji, M. Caricato, X. Li, H. P. Hratchian, A. F. Izmaylov, J. Bloino, G. Zheng, J. L. Sonnenberg, M. Hada, M. Ehara, K. Toyota, R. Fukuda, J. Hasegawa, M. Ishida, T. Nakajima, Y. Honda, O. Kitao, H. Nakai, T. Vreven, J. A. Montgomery Jr, J. E. Peralta, F. Ogliaro, M. Bearpark, J. J. Heyd, E. Brothers, K. N. Kudin, V. N. Staroverov, R. Kobayashi, J. Normand, K. Raghavachari, A. Rendel, J. C. Burant, S. S. Iyengar, J. Tomasi, M. Cossi, N. Rega, N. J. Millam, M. Klene, J. E. Knox, J. B. Cross, V. Bakken, C. Adamo, J. Jaramillo, R. Gomperts, R. E. Stratmann, O. Yazyev, A. J. Austin, R. Cammi, C. Pomelli, J. W. Ochterski, R. L. Martin, K. Morokuma, V. G. Zakrzewski, G. A. Voth, P. Salvador, J. J. Dannenberg, S. Dapprich, A. D. Daniels, Ö. Farkas, J. B. Foresman, J. V. Ortiz, J. Cioslowski, D. J. Fox, Gaussian 09, Revision A.02, Gaussian, Inc.: Wallingford, CT, 2009.

(14) A. Hasija, R. Bhowal, D. Chopra, Quantitative Investigation of Weak Intermolecular Interactions of −F and −CF3 Substituted in Situ Cryocrystallized Benzaldehydes, *Cryst. Growth Des.* 2020, **20**, 7921.

(15) Gavezzotti, A. (2003). *Calculation of Intermolecular Interaction Energies by Direct Numerical Integration over Electron Densities. 2. An Improved Polarization Model and the Evaluation of Dispersion and Repulsion Energies.* The Journal of Physical Chemistry B, 107, 2344–2353.

(16) Gavezzotti, A. (2005). *Calculation of lattice energies of organic crystals: the PIXEL integration method in comparison with more traditional methods*. Zeitschrift Für Kristallographie - Crystalline Materials, 220, 499-510.

(17) Gavezzotti, A. (2013). *Equilibrium structure and dynamics of organic crystals by Monte Carlo simulation: critical assessment of force fields and comparison with static packing analysis.* New Journal of Chemistry, 37, 2110-19.

(18) Stephenson, Richard M.; Malanowski, Stanislaw, Handbook of the Thermodynamics of Organic Compounds, 1987, https://doi.org/10.1007/978-94-009-3173-2.

(19) L. J. Bellamy, R. J. Pace, Hydrogen bonding in carboxylic acids-I. Oxalic acids, *Spectrochim. Acta* 1963, **19**, 435.

(20) Q. X. Ma, H. He, C. Liu, Hygroscopic properties of oxalic acid and atmospherically relevant oxalates, *Atmos. Environ.* 2013, **69**, 281.

(21) González-González, J. S.; Martínez-Martínez, F. J.; Peraza-Campos, A. L.; Rosales-Hoz, M. J.; García-Báez, E. V.; Padilla-Martínez, I. I. Supramolecular architectures of conformationally controlled 1,3-phenyl-dioxalamic molecular clefts through hydrogen bonding and steric restraints. *CrystEngComm* **2011**, *13*, 4748-4761.

(22) González-González, J. S.; Martínez-Martínez, F. J.; García-Báez E. V.; Cruz, A.; Morín-Sánchez, Luis M.; Rojas-Lima, S.; Padilla-Martínez, I. I., Molecular Complexes of Diethyl N,N′-1,3-Phenyldioxalamate and Resorcinols: Conformational Switching through Intramolecular Three-Centered Hydrogen-Bonding. *Cryst. Growth Des.* **2014**, *14*, 628-642.